AN ABSTRACT OF THE THESIS OF

D.K. Ravi for the degree of Master of Science in Electrical and Computer Engineering presented on June 8, 1992.

Title : Design Studies Relating to the Brushless Doubly-Fed Automotive Alternator

Abstract approved : _____ René Spée

The alternators in today's automobiles are of the claw-pole or Lundell construction, which is a readily manufactured, low-cost derivative of the conventional rotating dc field synchronous generator. The efficiency of the Lundell system is low due to a complicated magnetic circuit of predominantly solid steel and a high windage rotor structure. As the number of electrical devices in a car increases, so does the demand on the generator system. The Lundell alternator is not able to meet the demands and numerous alternative systems are under investigation. This led to the development of the brushless doubly-fed alternator system with the advantages of regulation over a wide speed range, competitive system cost based on inexpensive machine construction, low rating controller, diode rectifier and robust, low maintenance configuration.

The conventional alternator has only one degree of control (dc excitation), whereas the doubly-fed alternator has three control quantities: excitation magnitude, frequency and phase sequence. Excitation magnitude is used to regulate the output voltage, which leaves

two control parameters to optimize efficiency over the alternator speed range. Simulation tools were developed for conducting design studies on the BDFM alternator system. Various stator and rotor configurations were studied through simulation and a few prototypes were built.

A proof-of-concept prototype built in an existing induction machine frame achieved comparable efficiency characteristics to the Lundell System and exceeded the Lundell performance over part of the speed range. Significant performance improvements are expected for a new, optimized prototype which will not rely on the induction machine laminations, but will utilize custom components designed for this low voltage, high frequency application.

Since the increase in automotive power demand is likely to be coupled with an increase in system voltage, a 24V, 2kW alternator system is investigated and simulation results are presented.

Design Studies Relating to the Brushless Doubly-Fed Automotive Alternator

by

D.K. Ravi

A THESIS

submitted to

Oregon State University

in partial fulfillment of
the requirements for the
degree of

Master of Science

Completed June 8, 1992

Commencement June 1993

APPROVED:

Redacted for privacy

Assistant Professor of Electrical and Computer Engineering in charge of major

Redacted for privacy

Head of Department of Electrical and Computer Engineering

Redacted for privacy

Dean of Graduate School

Date of thesis presentation June 8, 1992

Typed by D.K. Ravi

ACKNOWLEDGEMENTS

I would like to thank Dr. René Spée for his invaluable guidance, support and enthusiasm for this project. I would also like to thank Dr. G.C. Alexander, Dr. Mario Magana and Dr. Youngshun Chen (GCR) for being on my graduate committee. Special thanks to Dr. G.C. Alexander for his review and feedback on the thesis. Thanks also to Dr. Alan K. Wallace for his assistance during the early part of my thesis work.

Thanks to my colleagues for their help in various ways during the development of this thesis. Special thanks to Patrick Rochelle for getting me started on the BDFM simulation program and to Virendra Javedakar for testing the machines in the laboratory. Also thanks to all my friends here who made my stay in school a pleasant, fun filled one. And last but not the least, I would like to thank my family back home for their support and encouragement.

ACKNOWLEDGEMENTS

The work described in this thesis has been supported by a consortium consisting of Bonneville Power Administration, Puget Sound Power and Light, and Electric Power Research Institute. The author is appreciative of the funding which made this work possible.

TABLE OF CONTENTS

LIST OF FIGURES

LIST OF TABLES

Design Studies Relating to the Brushless Doubly-Fed Automotive Alternator

CHAPTER 1

INTRODUCTION

The brushless doubly-fed machine (BDFM) is based on the concept of self-cascaded induction machines, with two stator windings of different pole numbers and a nested-cage rotor structure. The stator structure can be realized by two physically separate windings or by a single winding connected for two different pole numbers [1]. The BDFM in conjunction with a converter can be used in an adjustable speed drive (ASD) system or in variable speed generation (VSG) applications.

Most ASD systems today are squirrel-cage induction machines controlled by a variable frequency - variable voltage converter. In this configuration (Fig. 1.1a), the power converter has to be rated at about 115% of the induction machine, since the converter supplies electro-mechanical power as well machine and semiconductor losses. The cost per installed kVA for the converter is substantially higher than that for the machine. Thus, the resulting ASD system cost can be quite high. In some ASD applications, the wound-rotor induction machine is used. The drawback of this configuration is the high cost of the wound-rotor machine. Another detriment lies in the maintenance of slip rings and brushes that are required for speed control.

In ASD applications, the BDFM is an attractive alternative to the above systems, due to the robust machine construction and reduced overall system cost (machine cost + power electronics cost). The rating of the power converter in the BDFM system (Fig. 1.1b) is a fraction of the rating of the machine, leading to a reduction in system cost.

In a VSG system configuration [2], the BDFM system has the advantage of having AC excitation rather than DC excitation, as in a conventional synchronous machine system, to control the output voltage at different speeds. The AC excitation allows for

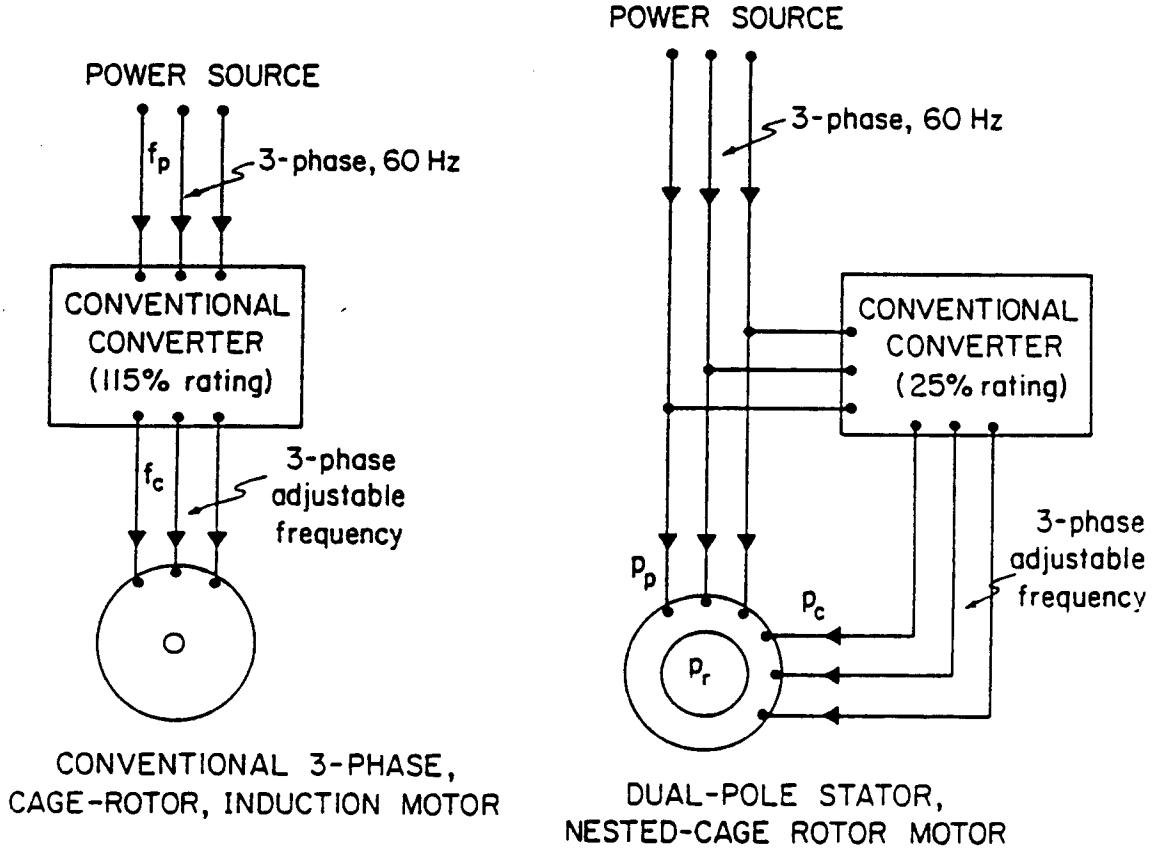

Fig. 1.1a Conventional induction machine adjustable speed drive

1.1b Brushless doubly-fed drive system

three degrees of control: magnitude, frequency and phase sequence. Since only one parameter is required for controlling the output voltage, the other parameters can be used to control other system performance parameters. Depending on the application, this could be output frequency, efficiency or power factor. For example, in automotive alternator applications, efficiency at all speeds is of primary importance.

Much of the work reported in this thesis relates to the design of an efficient automotive alternator capable of maintaining a reasonably high efficiency at speeds ranging from 2000 r/min to 6000 r/min and while supplying varying electrical loads.

The automotive alternators in use today are of the claw-pole Lundell type of construction (Fig. 1.2), which is a robust derivative of the rotating DC field synchronous generator. Although this construction provides for simple means of controlling the DC current flowing in the rotor coils to control the output voltage (Fig. 1.3) at varying speeds, it has some serious drawbacks [3]:

1. The magnetic field has to pass axially through the magnetic core and shaft. Hence, increasing the power rating of the machine can only be achieved by increasing the rotor diameter. Given the projected increase of automotive alternator rating and the space constraints under the hood, increasing the machine size is not always possible.
2. The solid claw-pole structure of the rotor gives rise to eddy current losses in the rotor. This heats up the rotor coils, thereby reducing the rating of the coil and bringing down the overall efficiency.

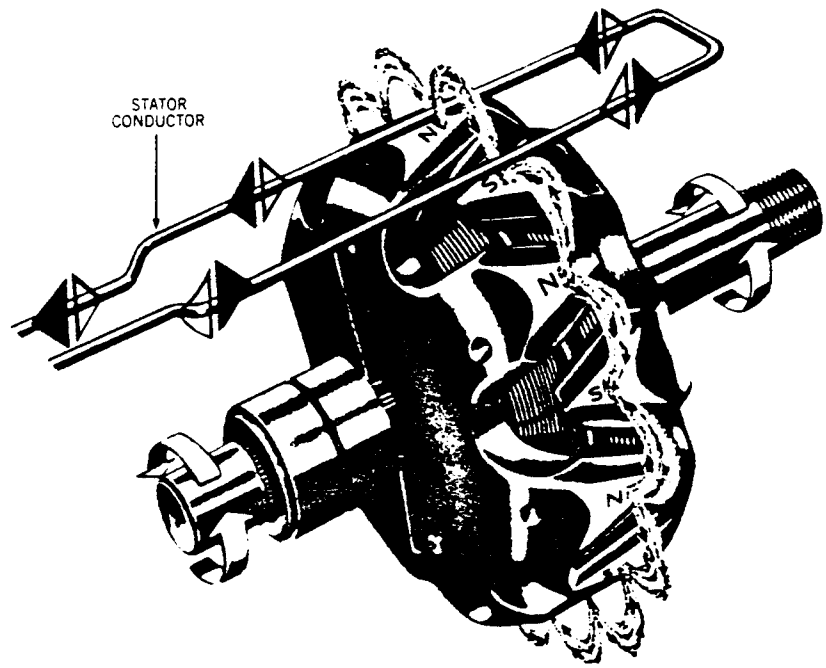

Fig. 1.2 Rotor structure of the Lundell machine [23]

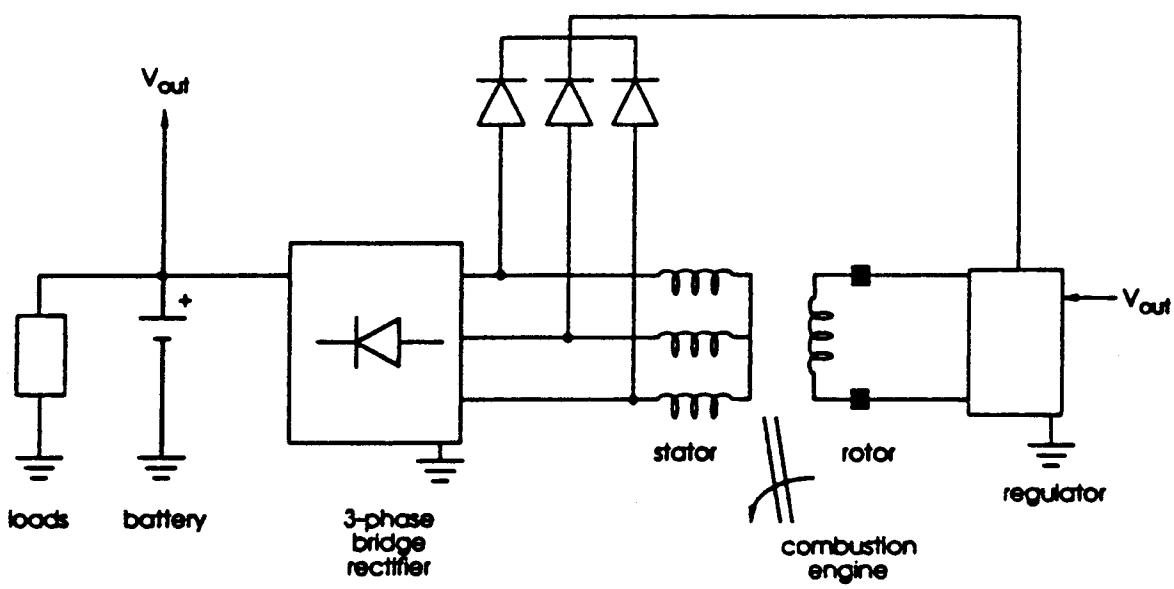

Fig. 1.3 Lundell alternator system [2]

Because of these drawbacks various alternative automotive alternator systems have been proposed. Mhango [4] has proposed a reduction of the speed range by use of a gear box or adjustable pulleys to increase the efficiency of the Lundell alternator. But these techniques increase the system cost, reduce reliability and complicate the control system. Wang and Demerdash [5] have published highly detailed finite element analysis on the Lundell alternator, but the findings result in very high per unit cost systems, which are not desirable for automotive applications. Others have proposed using an inherently more efficient machine for generation. Recent advances in permanent magnet materials have resulted in high performance brushless DC machines which can be used as automotive alternators and motors [6]. Even though these machines would probably be the best in efficiency, there are some serious drawbacks to their applications in an automotive environment:

1. High per unit cost because of expensive permanent magnets.
2. Permanent magnet deterioration because of thermal, mechanical and corrosive properties of the magnetic material.
3. Large controllable power converter for voltage regulation.

A BDFM variable speed generation system has the advantages of output voltage regulation over wide speed ranges, inexpensive and robust machine construction, low rating controller and uncontrolled diode rectifier. Consequently, system cost is very competitive and the BDFM seems a viable alternative for future automotive alternators. The possibility of upgrading the BDFM system voltage without much difficulty to a 24V or a 36V system, which might become the future alternator standard, should also weigh

in favor of the BDFM alternator system.

A detailed simulation program based on the generalized version developed by Rochelle [7] has been modified for this thesis to accommodate various stator and rotor configurations. Also, the available d-q and steady state models [8] were used extensively for designing the automotive BDFM alternator. The remaining chapters in this thesis give details about the operating principles of the BDFM and the design procedures developed.

1.1 Literature Review:

The concept of using two cascade connected induction machines for speed control is not new. However, since two separate wound rotor induction machines are required, total system cost becomes very high. In 1907, Hunt [1] proposed a self cascaded induction machine with two windings on the stator and a special rotor configuration. The two three phase windings on the stator are of different pole numbers. Speed control was achieved by connecting one set of three phase windings to the power grid and the second set to a bank of resistors. Creedy [9] refined the BDFM design and developed a rotor which would support the currents induced by the two stator windings. He detailed the design of a 6 pole and 2 pole machine. Broadway [10] made further advancements to the rotor design by proposing a simple squirrel cage loop structure. He also developed general performance equations and a steady-state equivalent circuit for the BDFM. The basic loop structure of the rotor suggested by Broadway is the building block of the rotor investigations discussed in this thesis.

With the advent of power electronic converters, Cook and Smith [11] and Kusko and Somah [12] developed methods to study the dynamic performance of a BDFM operated in the induction mode (slip-power pumped back to the system) and in the synchronous mode, a mode of operation which requires the excitation of both the stator windings. The various modes of operation of the BDFM will be explained in the next chapter.

The drawback of most published analyses is that they consider the BDFM as two separate wound induction machines connected in cascade. Further they assume ideal sinusoidal windings which is untrue in self cascaded machines - particularly for the higher pole number windings. The models developed from these assumptions are adequate for steady-state performance analysis and within limits, for stability studies. However, for detailed design and stability studies more precise models are required.

Wallace et. al.[13] developed a detailed simulation model which gives time domain analysis of the stator and rotor currents, the mechanical speed and the torque developed in the machine. Rochelle et. al.[14,15] used the detailed program to investigate various stator and rotor configurations of the BDFM and their effects on machine performance in ASD applications. In these investigations, the stator and rotor structure in terms of pole numbers of the two windings and the number of nests in the rotor remained the same. The results of the detailed model were used for field analysis of the BDFM by Alexander [16], who also verified the detailed model results independently.

For control studies the detailed model is too complicated. Thus, Li [8] reduced the

higher order model to a simplified two-axis (d-q) model. In turn, simplification of the d-q model leads to a steady-state model [17]. Methods to calculate d-q and steady-state model parameters from a-b-c domain parameters were also developed. Unlike for conventional induction machines, these calculations are not very straightforward for the BDFM due to the different pole numbers present.

Lauw et. al.[18] suggested using the BDFM in conjunction with a series resonant converter in a VSG system. His experiments were carried out on a wound rotor induction machine, with the resonant converter connected to the rotor through the slip rings. The philosophy of these experiments can be extended to a BDFM with a cage / loop rotor and with the converter connected to the second set of stator windings.

CHAPTER 2

BDFM PRINCIPLES AND DESIGN TOOLS

The BDFM is essentially a single unit version of two separate induction machines connected in cascade. In construction, however, the BDFM resembles the conventional induction machine with a few changes. This chapter explains the operating principles of the BDFM and reviews the design tools that were developed.

The stator of a BDFM has two sets of three phase windings wound for different pole pairs. In this thesis, the two three phase windings will be referred to as power winding (p_p pole pairs) and control winding (p_c pole pairs). This can be achieved by having a common winding, wherein an ingenious [1,9,14] way of coil connection will result in two sets of three phase terminals, as illustrated in Figure 2.1. However, this connection gives rise to circulating currents in the coil groups of a phase [16], which causes deterioration of machine performance. This encourages the use of isolated windings, where two separate three phase windings are wound on the same stator frame, as shown in Figure 2.2. Since the two stator windings are of different pole numbers, ideally there is no direct mutual coupling and frequency separation is maintained.

When the power and control windings are excited by balanced three phase voltages of frequencies f_p and f_c respectively, then the air-gap magnetomotive force (mmf) is given by the expression [19]

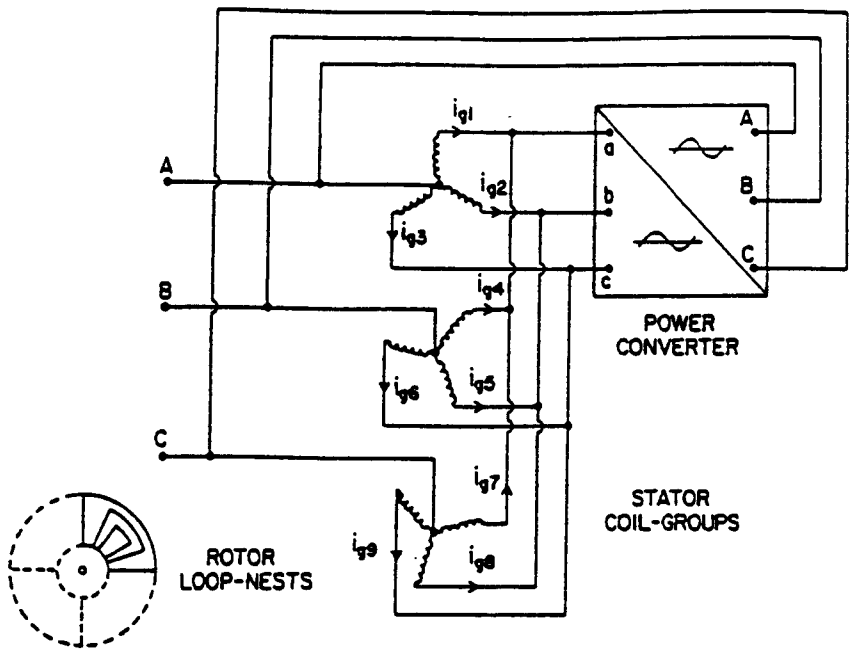

Fig. 2.1 BDFM system - Common winding [19]

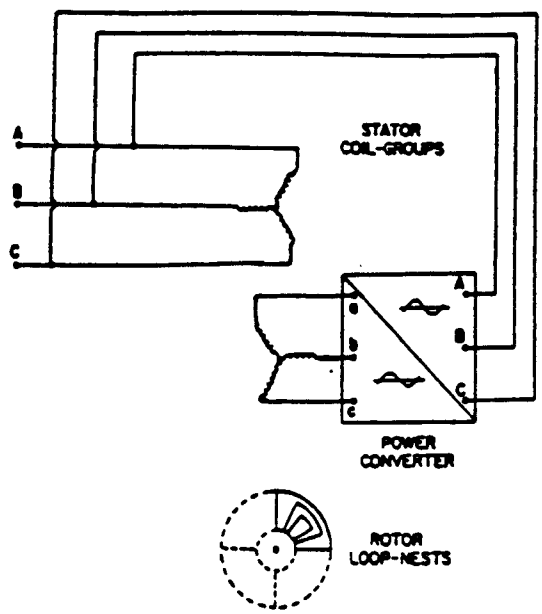

Fig. 2.2 BDFM system - Isolated windings [19]

$$MMF_p = k_p I_p (3/2)\sin(\omega_p t - p_p \Theta_s) \quad \text{-- 2.1}$$

$$MMF_c = k_c I_c (3/2)\sin(\omega_c t - p_c \Theta_s) \quad \text{-- 2.2}$$

where MMF_p and MMF_c are the mmf produced by the power and the control winding when excited separately, k_p and k_c are the peak equivalent number of turns, I_p and I_c are the peak currents, ω_p and ω_c are the frequencies in rad/s and p_p and p_c are the number of pole pairs of the power and control winding, respectively. Θ_s is the stator angle in radians. Figure 2.3 shows the mmf pattern for a $p_p = 3$ and $p_c = 1$ pole-pair, double-layer winding with 1 turn/coil.

Considering a linear magnetic circuit and applying superposition, the net stator air-gap mmf, can be obtained by adding equations 2.1 and 2.2, as illustrated in Figure 2.4. This pattern is at a particular instant in time and for unit current, the pattern will change with time and current magnitudes. Reference [19] has more details on this analysis.

For the BDFM to be able to operate in the synchronous mode, the rotor must be able to support the fields produced by both the power and the control winding. This has led to the development of the nested loop rotor design by Broadway[10], as illustrated in Figure 2.5. The number of nests in the rotor has to be equal to the sum of power and control winding pole pairs. Mathematically; $p_r = p_p + p_c$, where p_r is the number of nests in the rotor.

As mentioned earlier, the rotor has to support the fields produced by both the power and the control winding. Furthermore, for synchronous operation the currents induced in

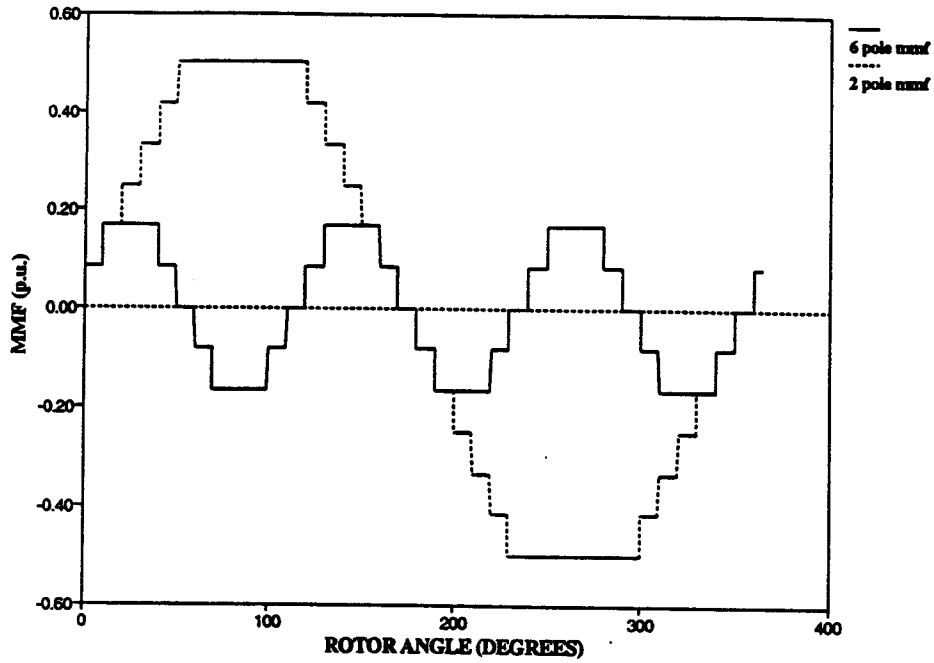

Fig. 2.3 MMF pattern for a double layer, 1 turn/coil 6 pole and 2 pole winding.

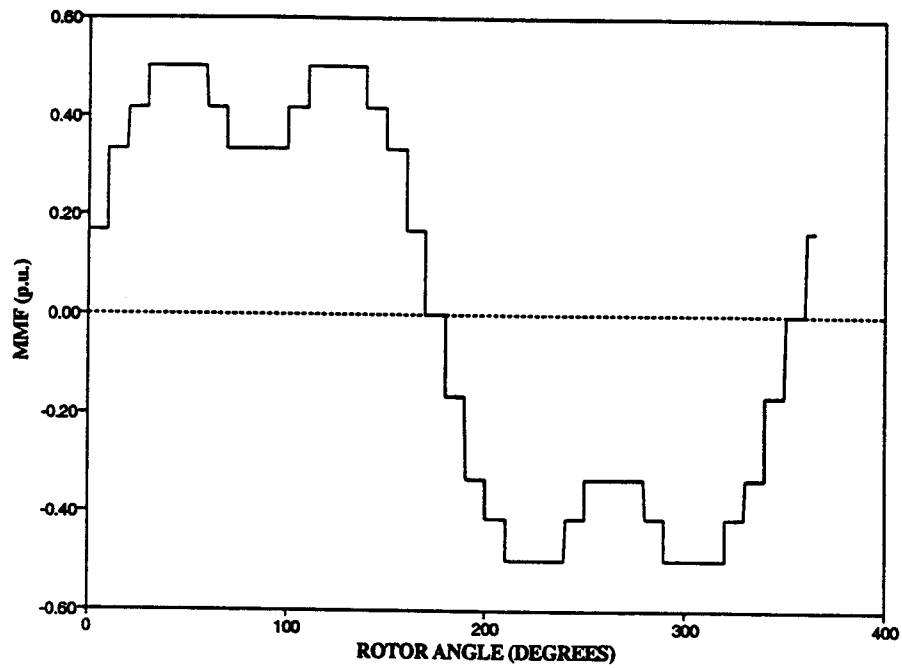

Fig. 2.4 MMF pattern in air-gap due to stator.

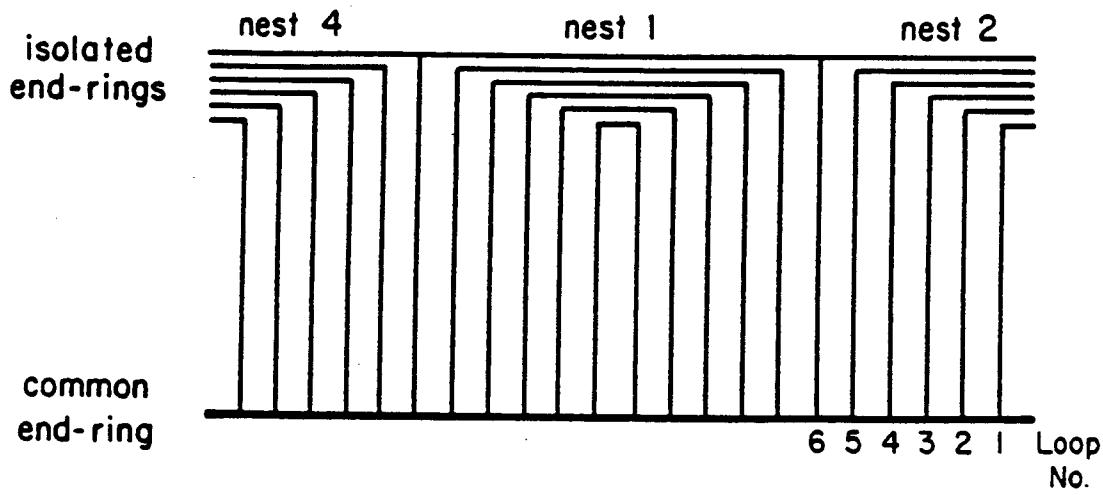

Fig. 2.5 Broadway cage/loop rotor [15]

the rotor should be of a single frequency. To illustrate this, the BDFM can be considered as two separate induction machines of p_p and p_c pole pairs, the rotors of which are coupled electrically as well as mechanically[2,17]. The p_p machine (representing the power winding) is excited with a three phase supply of frequency f_p and the p_c machine (representing the control winding) is excited with a frequency of f_c. The control winding phase sequence may be different from the phase sequence of the power winding. If the rotor is rotating at a speed ω_r in the direction of the power winding field, then the power and the control winding will induce currents in the rotor of frequency ω_{pr} and ω_{cr}[19]. This is illustrated in Figure 2.6. From this figure the following equations can be derived;

$$\omega_{pr} = \omega_p - \omega_r \qquad \text{-- 2.3}$$

$$\omega_{cr} = \pm\omega_c + \omega_r \qquad \text{-- 2.4}$$

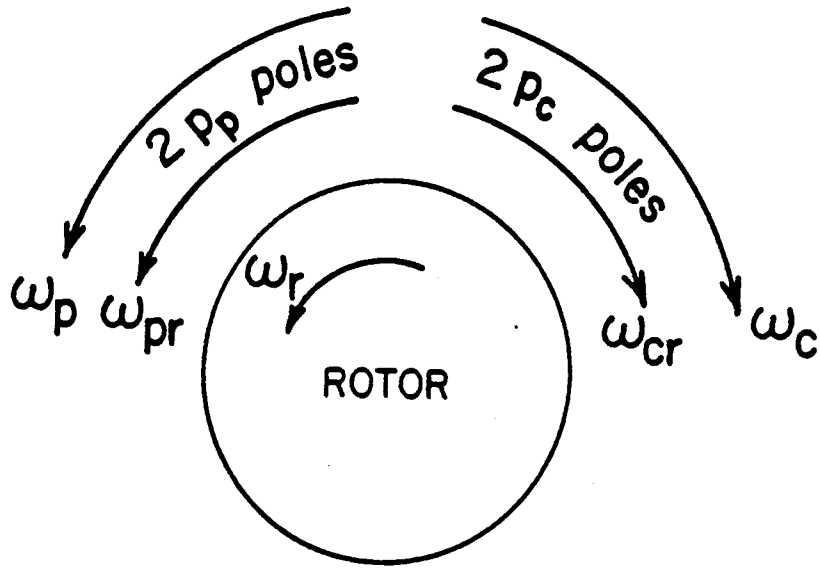

Fig. 2.6 Rotational angular velocities in the BDFM [2]

where $\omega_p = \frac{2\pi f_p}{p_p}$ and $\omega_c = \frac{2\pi f_c}{p_c}$

The $\pm\omega_c$ in equation 2.4 indicates the phase sequence of the control winding supply with respect to the power winding; a positive control winding sequence is opposite to the power winding phase sequence.

For synchronous operation of the BDFM, the rotor currents should be of a single frequency, f_r. Applying this to equations 2.3 and 2.4 yields,

$$\frac{2\pi f_r}{p_p} = \frac{2\pi f_p}{p_p} - \omega_r \qquad \text{-- 2.5}$$

$$\frac{2\pi f_r}{p_c} = \frac{\pm 2\pi f_c}{p_c} + \omega_r \qquad \text{-- 2.6}$$

Eliminating f_r from equations 2.5 and 2.6 and solving for ω_r, gives

$$\omega_r = \frac{2\pi(f_p - (\pm f_c))}{p_p + p_c} \qquad \text{-- 2.7}$$

The BDFM is said to operate in the synchronous mode when equation 2.7 is satisfied. All other modes of operation are termed the induction mode.

2.1 Design and Simulation Tools:

The previous section established the basic operating principles of the BDFM. The next step in the design process of the BDFM would be to develop a thorough understanding of the electrical and mechanical characteristics of the BDFM. To this effect a dynamic simulation program was developed by Spee et.al.[13].

The first simulation program, Program BDFM [7], modelled a 36 slot stator and a 44 bar rotor. The dimensions of the machine are an input to the program and are required to calculate the machine parameters. The stator windings consists of a $2p_p = 6$ pole power winding and a $2p_c = 2$ pole control winding. The rotor consists of four symmetrical nests

with 6 loops/nest. The machine equations are written in state variable form, where the machine currents form the electrical states. The currents of the two three phase stator windings comprise the first 6 states and the currents of the 24 rotor loops (4 nests * 6 loops/nest) comprise the remaining states in the current vector. A brief discussion on the development of the state equations follows. A detailed development is in reference [7].

Kirchoff's Voltage Law is applied to all 30 loops (6 stator loops + 24 rotor loops). The equation in matrix form is

$$[V] = [Z][I] \qquad \text{-- 2.1.1}$$

where [V] is the input voltage vector, [Z] is the machine impedance matrix and [I] is the state vector (machine current vector). For any coil j, the general form of the voltage equation is [7]

$$v_j = r_j i_j + \sum_{\substack{j=1 \\ j\neq k}} r_{jk} i_k + l_j p i_j + p \sum_{\substack{j=1 \\ j\neq k}} (M_{jk} i_k) \qquad \text{-- 2.1.2}$$

where v_j is the input voltage of coil j, r_j and l_j are the resistance and self inductance of coil j, r_{jk} and M_{jk} are the mutual resistance and mutual inductance between coil j and coil k. Here, mutual resistance refers to the common resistance between coil j and coil k, which is non-zero for the loop bars comprising the cage. In equation 2.1.2, p is the differential operator.

Applying the chain rule for partial differentiation to the above equation and then writing the equation in matrix form[7]

$$[V] = ([R] + \omega_r * [\partial M/\partial \Theta_r] + [M]p)[I] \qquad \text{-- 2.1.3}$$

This equation describes the electrical system. The mechanical system is modelled by a second-order equation:[7]

$$p\omega_r = (1/J)(T_e - T_l + B\omega_r) \quad \text{-- 2.1.4}$$

$$p\Theta_r = \omega_r \quad \text{-- 2.1.5}$$

where J is the inertia of the load and the rotor, ω_r is the shaft speed of the rotor, T_l is the load torque and T_e is the electromagnetic torque; B is the viscous damping coefficient and Θ_r is the angular position of the rotor.

For solving the above equations all the machine parameters (resistances and inductances) should be known. These calculations are discussed in reference [13] and the programming implementation of these equations is explained in reference [7]. A simplified flowchart for Program "BDFM"[7] is shown in Figure 2.1.1.

The output of this detailed program gives the stator phase currents and all the rotor loop currents as well as the torque contributions by the individual windings. This information can be used for design studies on the BDFM.

Program "BDFM" originally was machine specific, i.e. the program was written for a particular machine with a specific stator and rotor geometry. To investigate machine performance with different stator and rotor geometries, a generalized version of Program "BDFM" was developed by Rochelle[7]. The generalized program was modified and used extensively for the design work presented in this thesis.

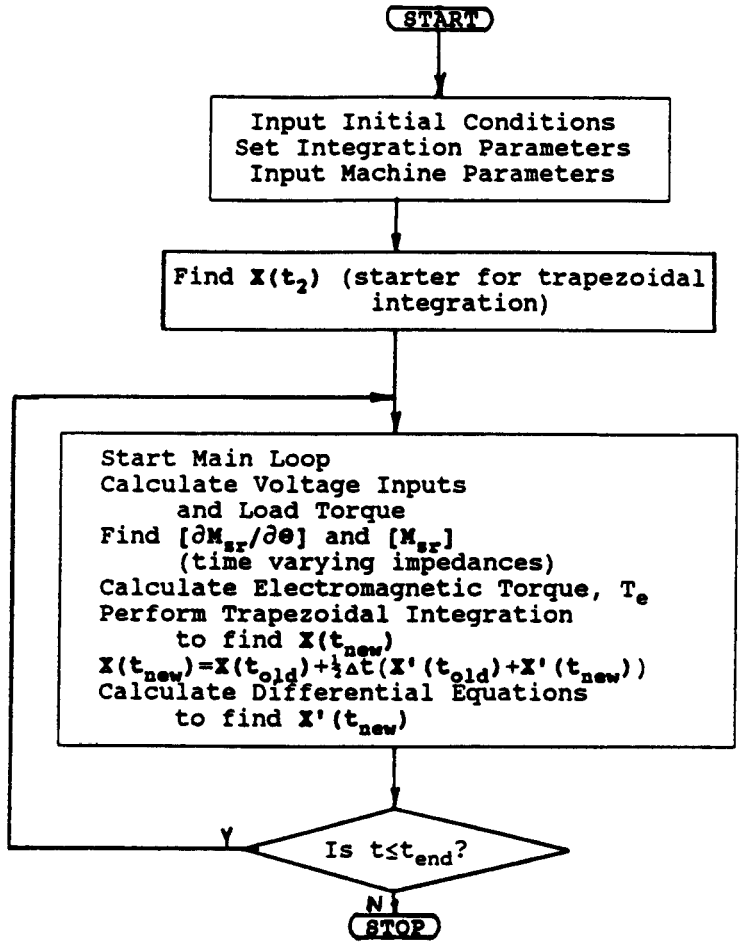

Fig. 2.1.1 Simplified flowchart for Program 'BDFM' [7]

Program BDFM and the generalized version are very detailed programs and help establish the basic operation of the machine but are of limited use as design tools. A reduced order model (d-q model) was developed by Li, et.al.[8,17] to facilitate dynamic and steady-state analysis and also conduct machine and control system design studies by correlating machine performance to machine parameters. Assuming balanced input voltages and neglecting zero sequence quantities, the d-q model is an 8^{th} order system. In

the rotor reference frame [17], the electrical equations can be written as:

$$\begin{bmatrix} v_{q6} \\ v_{d6} \\ v_{o6} \\ v_{q2} \\ v_{d2} \\ v_{o2} \\ v_{qr} \\ v_{dr} \end{bmatrix} = \begin{bmatrix} r_6+L_{s6}p & 3L_{s6}\omega_r & 0 & 0 & 0 & 0 & M_6p & 3M_6\omega_r \\ -3L_{s6}\omega_r & r_6+L_{s6}p & 0 & 0 & 0 & 0 & -3M_6\omega_r & M_6p \\ 0 & 0 & r_6+L_{l6}p & 0 & 0 & 0 & 0 & 0 \\ 0 & 0 & 0 & r_2+L_{s2}p & L_{s2}\omega_r & 0 & -M_2p & M_2\omega_r \\ 0 & 0 & 0 & -L_{s2}\omega_r & r_2+L_{s2}p & 0 & M_2\omega_r & M_2p \\ 0 & 0 & 0 & 0 & 0 & r_2+L_{l2}p & 0 & 0 \\ M_6p & 0 & 0 & -M_2p & 0 & 0 & r_r+L_rp & 0 \\ 0 & M_6p & 0 & 0 & M_2p & 0 & 0 & r_r+L_rp \end{bmatrix} \begin{bmatrix} i_{q6} \\ i_{d6} \\ i_{o6} \\ i_{q2} \\ i_{d2} \\ i_{o2} \\ i_{qr} \\ i_{dr} \end{bmatrix}$$

which suggests the equivalent circuit as shown in Figure 2.1.2. References [8,17] have more details on the development of the d-q model.

Design studies for an automotive alternator were performed by using the steady-state model[17], which can be derived from the d-q model. Since, in the d-q domain all the quantities have the same slip frequency s_1, ($s_1 = (\omega_6 - 3\omega_r)/\omega_6 = (\omega_2 + \omega_r)/\omega_6$), the differential operator p in equation 2.1.6 can be replaced by $j(\omega_6 - 3\omega_r)$ or by $j(\omega_2 + \omega_r)$. This results in the following steady-state equations[17]

$$V_{q6} = (r_6 + jX_{s6})i_{q6} + jX_{m6}i_{qr} \qquad \text{-- 2.1.7}$$

$$V_{q2} = (r_2 + sjX_{s2})i_{q2} - sjX_{m2}i_{qr} \qquad \text{-- 2.1.8}$$

$$V_{qr} = (r_r + s_1jX_r)i_{qr} + s_1jX_{m6}i_{q6} - s_1jX_{m2}i_{q2} \qquad \text{-- 2.1.9}$$

where V_{q6}, V_{q2}, V_{qr}, i_{q6}, i_{q2}, i_{qr} are all phasor quantities and slip $s= \omega_2/\omega_6$.

Further, $X_{s6} = \omega_6L_{s6}$, $X_{s2} = \omega_6L_{s2}$, $X_r = \omega_6L_r$, $X_{m6} = \omega_6M_6$ and $X_{m2} = \omega_6M_2$.

These equations lead to the steady-state equivalent circuit of Figure 2.1.3.

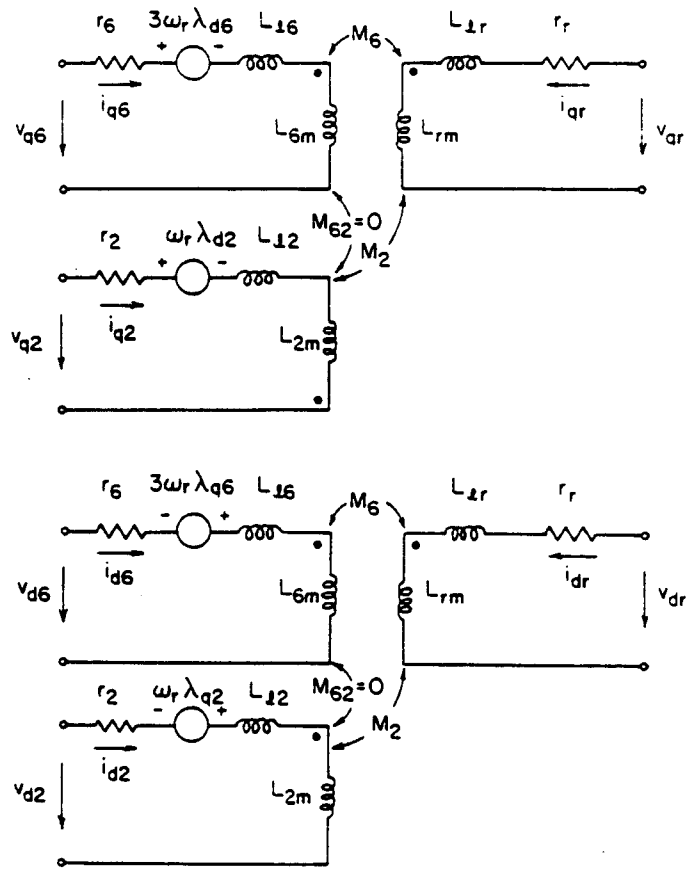

Fig. 2.1.2 Two-axis equivalent circuit of the BDFM [8]

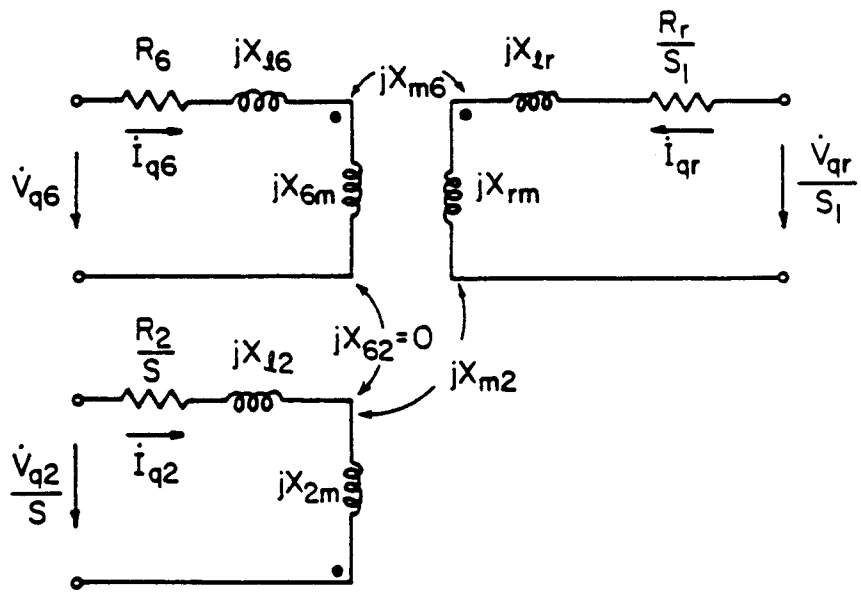

Fig. 2.1.3 Steady state equivalent circuit for synchronous operation [17]

CHAPTER 3

DESIGN OF A BDFM AUTOMOTIVE ALTERNATOR

This chapter details how the dynamic simulation program and the steady-state equivalent circuit are used for designing an alternator for automotive applications. After discussing the design procedure developed, various stator and rotor designs are presented. However, before addressing alternator design issues, a brief discussion of the BDFM alternator system is in order.

The BDFM alternator system configuration is shown in Fig. 3.1. The power winding of the BDFM is connected to a three phase diode rectifier to obtain a regulated dc output voltage (V_{dc}). Because of the low system operating voltage, it is essential that diodes with low forward drop be employed in the three phase rectifier. The rectifier output is connected to the battery (nominal voltage = 12V) and the loads are connected in parallel as shown in the figure. The alternator output voltage for a 12V system is required to be 14.5V [23] to charge the battery and supply the load requirements.

The control winding of the BDFM is connected to the output of a three phase PWM dc-ac inverter. The dc input to the inverter is from the dc output of the power winding. During start-up the inverter draws power from the battery. The inverter in the laboratory BDFM alternator set-up has 6 bipolar Darlington transistors for which the driving requirements are minimized by using complimentary devices in each leg of the three phase inverter. The PWM scheme is conventional, comparing a modulating sine wave

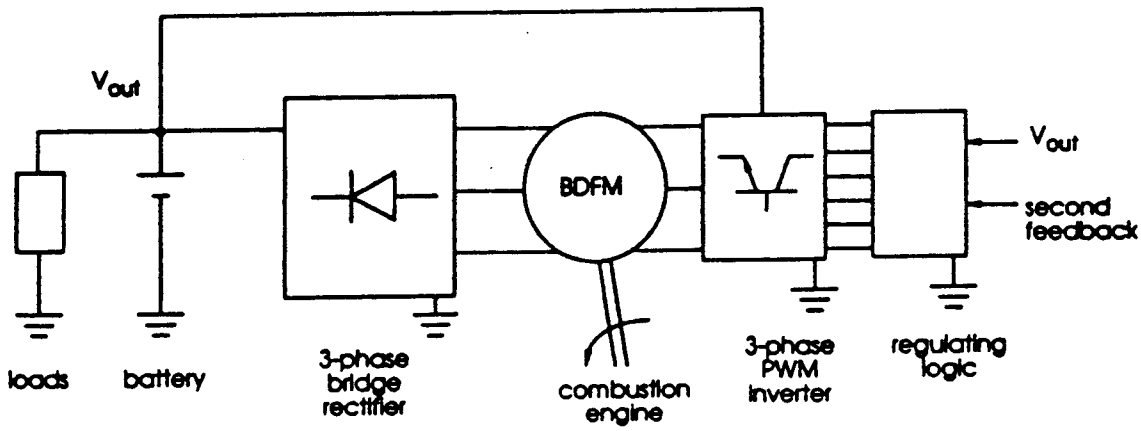

Fig. 3.1 BDFM alternator system

and a triangular carrier wave for controlling the transistors. Because of the dc input voltage limitation (equal to the battery voltage of 12V), the maximum ac line-to-line voltage output from the inverter operating in the square wave mode is approximately 8V. The expression for output voltage in the square wave mode is [20]

$$V_{ll(rms)max} = 0.78V_{dc}$$

Since the input dc voltage in the BDFM alternator system is 12V,

$$V_{ll(rms)max} = 0.78 \times 12 = 9.36v$$

However, during operation V_{dc} is 14.5V and the control winding voltage could be higher than 9.36V.

Because of a voltage drop of about 0.8V/transistor, the maximum available line-to-line output voltage is about 8V. The laboratory inverter performed satisfactorily over a wide range, [2v - 8v rms(line-to-line voltage), 5Hz - 200Hz, 0-15A] to provide the control winding with the required excitation. The control winding excitation should be such that the power winding generates 14.5V dc output at all load currents and battery conditions. However, the control winding excitation requirement should be kept to a minimum to reduce the inverter cost and thus the system cost. Regulation of the dc output voltage is achieved by a simple PI controller. Reference [21] has a more detailed explanation of the controller.

Since the BDFM alternator output is rectified, the frequency of the ac output need not be controlled to a particular value. The frequency of stator currents in the Lundell alternator varies from 700Hz to 280Hz as the speed varies from 6000r/min. to 2800r/min. The output frequency of the BDFM is derived from equation 2.7 in chapter 2.

$$f_p = (p_p + p_c)N_s \pm f_c \qquad \text{-- 3.1}$$

Equation 3.1 indicates that the power winding frequency is directly proportional to the sum of the power and control winding pole numbers. Equation 3.1 also indicates that the power winding frequency is less with a negative phase sequence control frequency (indicated by a "-" sign in the equation).

Because of the leakage and self inductance in the stator windings a high power winding frequency results in high reactive drop across the winding. Machine performance is adversely effected since this drop has to be compensated by generating a higher internal

voltage. In the BDFM generator system, the power winding frequency can be lowered by choosing a suitable power and control number of poles and by operating the control winding in the negative sequence. Prototype and simulation test results of a 3 pole pair power and 1 pole pair control winding are compared with a 6 pole pair power and 2 pole pair control winding machine in the following sections. The results indicate that the 3/1 pole pair machine performs well. The power winding frequency in this machine is almost half the frequency of the 6/2 pole pair machine. The results also indicate that the negative phase sequence control frequency gives better machine performance results.

3.1 BDFM Alternator Design Procedure

Two induction machine frames were considered for designing the prototype BDFM, a 1hp and a 2hp machine, both with 36 slot stators. The 1hp machine has 48 slots in the rotor. The rotor stampings of the 2hp machine were manufactured with 32 slots. The prototype BDFM machines were built around the available induction machine frames. Practical machine design needs to consider issues like stack length, stator slot depth, diameter and high frequency rotor design. The design requirements for the power winding of the BDFM alternator are: $V_{ll(rms)}$ = 11V, 40A dc load current.

The first step in designing a BDFM alternator is to decide on the number of poles on the power and control winding. Depending on the number of slots in the stator a single layer or a double layer winding is designed, based on conventional three phase distributed winding techniques. The rotor design starts with the decision on the type of cage/loop

structure: Broadway rotor, Broadway rotor without cage and interleaved rotor. The section on rotor design addresses this issue in detail. Once the basic alternator structure has been selected, the next issue is to decide on the number of turns on the power and the control windings. Initially one turn each on the power and control winding is considered. The generalized dynamic simulation program (explained in Chapter 2) is modified to accommodate the stator and rotor geometries. The generalized program calculates[7] all the stator phase resistances and inductances (both power and control winding) and all the rotor resistances and inductances (self inductance of all the loops and the mutual inductance between loops in a nest and between nests). The mutual inductances between a stator phase and all the loops in a nest of the rotor are calculated from a modified sub-routine of the generalized dynamic simulation program [7]. The phase quantities are then transformed to d-q circuit variables [8]. Thus, all the circuit parameters in the steady-state circuit (the resistance, self inductance and mutual inductance) are calculated. Appendix III explains the calculations of the parameters in detail. The steady-state circuit in the alternator configuration is shown in Fig. 3.1.1. The power winding is connected to the battery and load via the rectifier and the control winding is connected to the inverter as illustrated in the figure. Writing the steady-state equations from chapter 2 again for ease of explanation;

$$V_{q6} = (r_6 + jX_{s6})i_{q6} + jX_{m6}i_{qr} \qquad \text{-- 3.1.1}$$

$$V_{q2} = (r_2 + sjX_{s2})i_{q2} - sjX_{m2}i_{qr} \qquad \text{-- 3.1.2}$$

$$V_{qr} = (r_r + s_1jX_r)i_{qr} + s_1jX_{m6}i_{q6} - s_1jX_{m2}i_{q2} \qquad \text{-- 3.1.3}$$

$$s = \omega_2/\omega_6 \qquad \text{-- 3.1.4}$$

$$s_1 = (\omega_6 - 3\omega_r)/\omega_6 = (\omega_2 + \omega_r)/\omega_6 \qquad \text{-- 3.1.5}$$

and the expression for ω_6 from equation 3.1

$$\omega_6 = (p_p + p_c)N_s \pm \omega_c \qquad \text{-- 3.1.6}$$

N_s is the mechanical speed in rad/s and all the other quantities are as defined before.

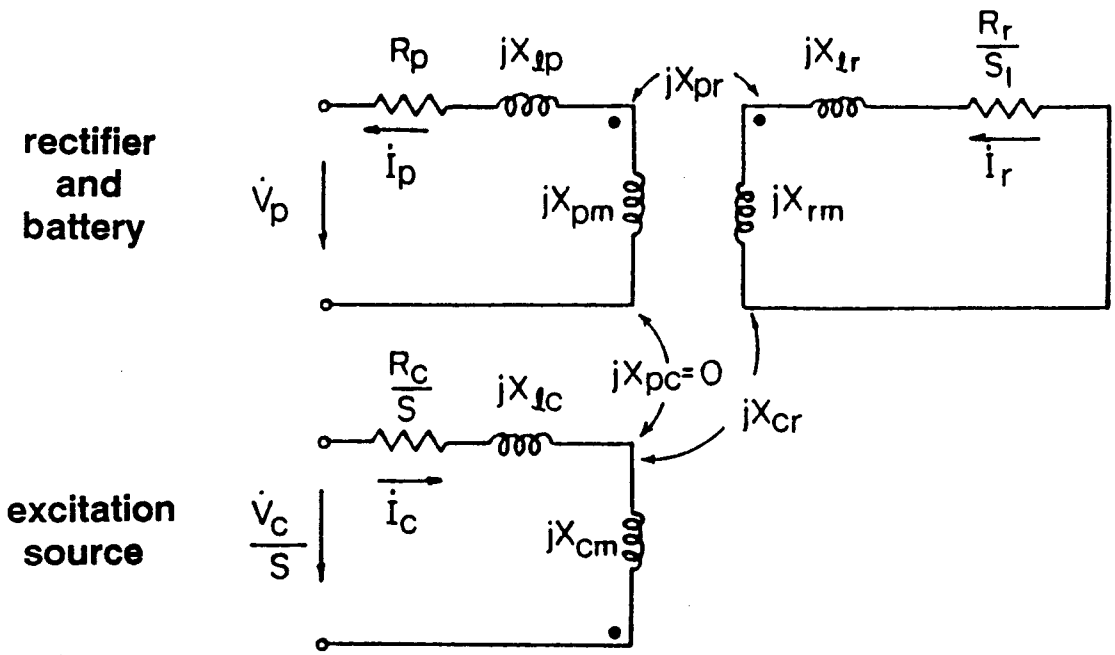

Fig. 3.1.1 Steady state circuit for alternator configuration

In the BDFM alternator, V_{q6} is known because the power winding is connected to a 12V battery through a rectifier and $V_{qr} = 0$, because of the short-circuited loops in the rotor. Further, the power factor between the power winding voltage and current approaches 0.955, assuming an uncontrolled three phase rectifier, continuous current flow and large machine output reactance (the displacement p.f. is very close to unity in this configuration)[20]. For a given operating point representing alternator speed and electrical load, the control winding excitation is calculated for a particular control frequency. Efficiency calculations are then performed. The excitation frequency is varied over a wide range (dc - 100Hz) and the best efficiency point is considered. All of these results

correspond to a single turn power and control winding on the stator. Refer to Appendix I for the steady-state program listing.

Design studies are performed by changing the number of turns on the power winding and control winding by correspondingly changing the resistance and inductance (self and mutual inductance). System efficiencies are calculated and then evaluated. Subsequently, this procedure can be performed for different stator (different pole numbers for power and control winding) and rotor configurations. The best BDFM design in a given frame is the configuration which has the best efficiency while having the excitation requirements at a minimum. A simplified flow-chart for the design procedure is shown in Fig. 3.1.2.

With the BDFM alternator design finalized, prototype machines were built and tested in the laboratory. The laboratory set-up shown in Fig. 3.1.3 uses a variable-voltage, variable-frequency inverter driven induction machine as prime mover. The speed of the prime mover can be changed from 0 to 50 r/sec and the speed of the alternator can be varied from 0 to 100 r/sec through the pulley arrangement (1:2 ratio). The set-up has a torque transducer which measures the torque and speed of the system, thus allowing the calculation of mechanical power. The alternator was tested at varying mechanical speeds and electrical loads and the performance compared to the predictions from the simulation model.

The next two sections describe the various stator and rotor configurations that were simulated and prototype machines built and tested in the laboratory.

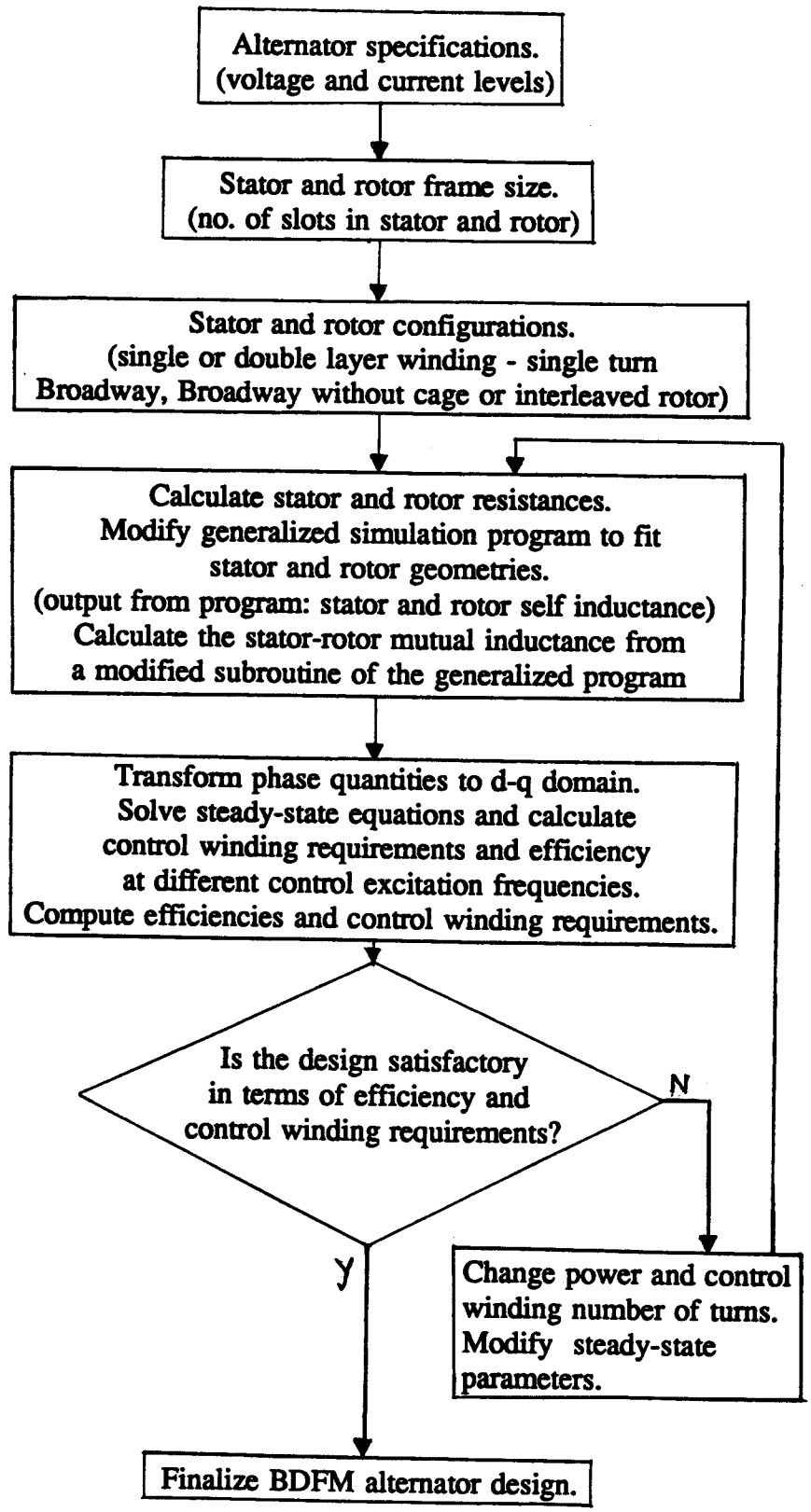

Fig. 3.1.2 Simplified flow-chart of the design procedure

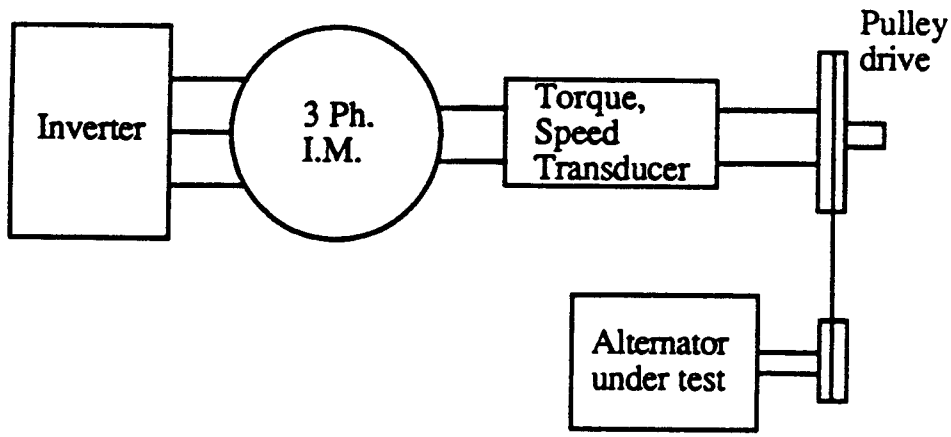

Fig. 3.1.3 Laboratory set-up for alternator testing

3.2 Stator Configurations

A first prototype BDFM alternator was constructed in a 1Hp induction machine frame. The stator had 36 slots and was wound for a 6 pole power and a 2 pole control winding. The rotor had 48 slots and had a Broadway cage rotor structure with 4 nests and 6 loops/nest. The performance of this machine was not good for a number of reasons. The stator slot area was very small and so the winding resistances of both the power and control winding were very high. The rotor core losses were very high due to the deterioration of the insulation between the stampings in the process of manufacturing the Broadway cage rotor. The rotor slots were also very small and of the closed, deep bar kind, leading to excessive resistive losses and high leakage inductance. All of this adversely effected machine performance in not being able to maintain charging voltage

(14.5V) at even low load currents of 10A. For this reason a second prototype was constructed in a 2hp induction machine frame. Rotor stamping for this machine were new and had good insulation between stamping. The details of the 2hp machine frame are as follows:

Stator stack length:	0.07m
Diameter at air-gap:	0.1125m
Air-gap length:	0.0005m
Number of stator slots:	36
Number of rotor slots:	32

To compare different stator configurations, the rotor configuration is the same; the Broadway cage rotor. Two different stator configurations were evaluated. The first prototype had a 6 pole power winding and a 2 pole control winding. The power and control winding were double-layer with 12 coils/phase. The stator winding layout for this machine is shown in Fig. 3.2.1. The rotor is a Broadway cage with 4 nests and 4 loops/nest. The other prototype constructed had a 12 pole power and a 4 pole control winding. Both the power and control winding were double-layer with 12 coils/phase . The rotor had 8 nests and 2 loops/nest. The parameters for the steady-state circuit of Fig. 3.1.1 are calculated for the machines according to the procedure described in the previous section. The resistance for the power and control winding on the stator and the loops in the rotor were calculated by considering the length of each coil and the wire gauge resistance from a wire table, corrected for the appropriate operating frequency. The wire gauge chosen should be such that the required number of turns can be accommodated in

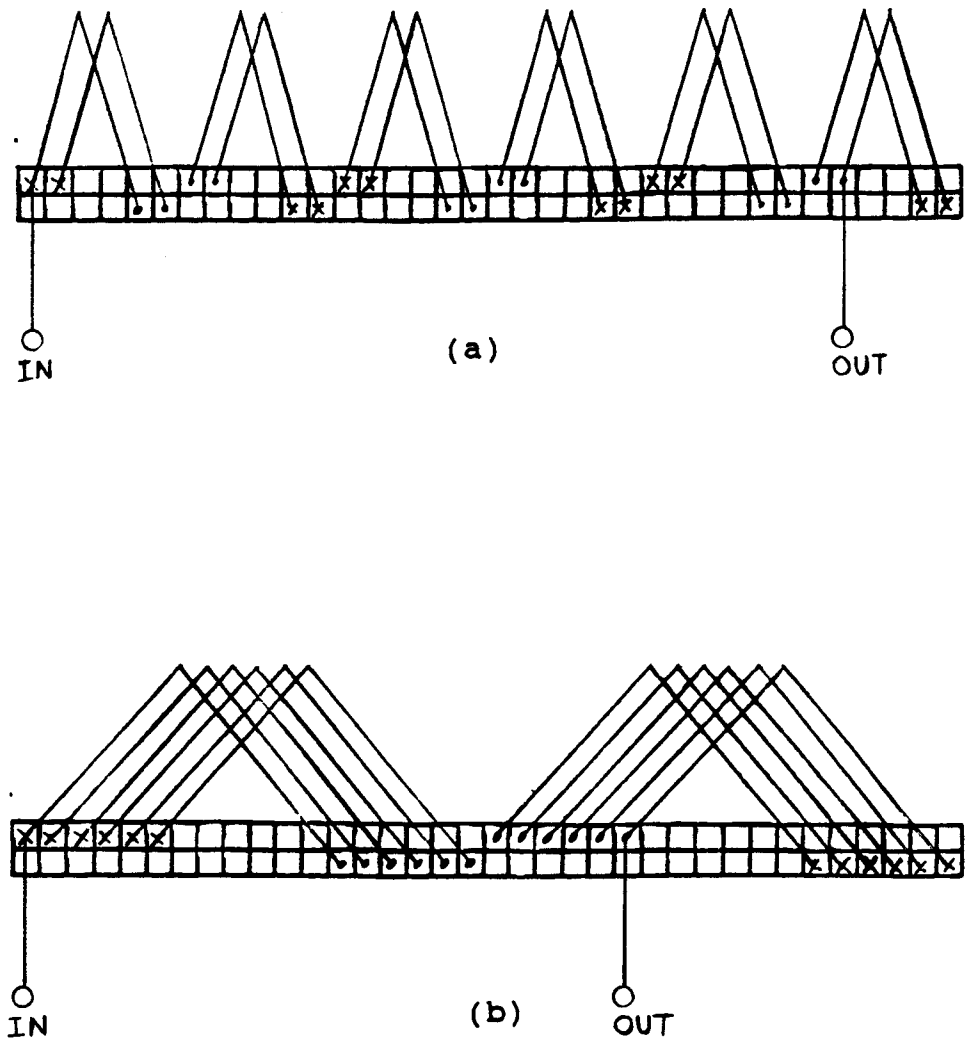

Fig. 3.2.1 Stator winding layout
(a) Six pole (phase A)
(b) Two pole (phase A)

the given slot area. The parameters for a single turn/coil power and control winding are listed in Table 3.2.1.

After calculating the parameters of the prototype machines, the steady-state equations are solved and the best stator configuration in terms of low control winding requirement and high system efficiency evaluated. These calculations were performed for two modes of excitation on the control winding:

1. The control winding phase sequence is opposite to the power winding phase sequence ($+f_c$) and
2. The control winding phase sequence is the same as power winding phase sequence ($-f_c$).

The excitation frequency was varied from dc to a maximum of 100Hz, depending on available dc link voltage. The steady-state model calculates the system efficiency and the control winding excitation requirement. Simulation studies were conducted for different electrical loads and alternator speeds. These tests were repeated for different stator configurations. Table 3.2.2 shows the results of the simulation program for a 6 pole power (1 turn/coil) and a 2 pole control (3 turns/coil) winding with a Broadway cage rotor. The results are for a dc output of 10A at $14.5V_{dc}$. The alternator speed is 6000r/min and the control winding excitation frequency varies from a very low value (almost dc) to 30Hz negative sequence. System efficiency is calculated by the expression below:

Efficiency = El. output/(El. output + total system losses),

where El. output = $V_{dc} * (I_{dc} - I_{inv})$. I_{inv} is the dc link current to the dc-ac PWM inverter.

Table 3.2.1
Steady-state parameters of the prototype machines
(power and control windings - 1 turn/coil, double layer)

Steady-state circuit parameters	Prototype machine 1 power wdg. - 6 pole control wdg.- 2 pole	Prototype machine 2 power wdg. - 12 pole control wdg.- 4 pole
R_p - Ω	0.022	0.030
L_{lp} - μH	20.0	39.600
L_{pm} - mH	0.225	0.224
M_{pr} - μH	38.885	21.279
R_c - Ω	0.020	0.0488
L_{lc} - mH	0.2	0.099
L_{cm} - mH	1.91	0.560
M_{cr} - mH	0.202	0.066
R_r - μΩ	240.0	185.0
L_{lr} - μH	2.995	1.010
L_{rm} - μH	26.954	9.111

Total system loss is calculated by adding all the losses listed below:

- Machine loss
  - Copper loss in the power, control and rotor windings.
  - Core loss is approximated by running the BDFM as an induction machine and finding the core loss at 60Hz and then extrapolating for the operating

frequencies of the BDFM.

- Windage loss is approximated by a cubic function of speed [4]. The fan constant for the BDFM will be lower than that of the Lundell machine because of the smooth rotor surface, the diameters being the same.

- Rectifier loss
  - This loss is calculated by multiplying the power winding current with the voltage drop in the diode bridge. The current flow in the bridge rectifier is such that two diodes are always conducting, so the loss can be approximated as $1.4 \times I_{pwd}$ W, considering a drop of 0.7V/diode. I_{pwd} is the power winding phase current.
- Inverter loss
  - This loss is similar to the rectifier loss but is associated with the control winding current. The loss is approximated as $2 \times I_{cwd}$ W, considering a drop of 1V per BJT. I_{cwd} is the control winding phase current.

Results similar to that in Table 3.2.2 were obtained for different stator configurations in terms of the number of turns/coil. Some of the different power and control winding configurations evaluated are: 2 turns/coil each on the two windings, 2 turns/coil on the power and 3 turns/coil on the control winding, 4 turns/coil on the power and 3 turns/coil on the control winding. Analyzing the predictions for the different stator configurations, the following observations can be made:

1. The alternator performance results are better when the phase sequence of the control winding is negative, i.e. the same as the power winding sequence.
2. The frequency of the control winding should be the maximum possible, given

the constraints of input dc link voltage and mechanical speed, for the best alternator performance.

3. A high number of turns/coil on the control winding is beneficial.
4. A low number of turns/coil on the power winding is desirable.

Laboratory tests were conducted on the 6 pole power (1 turn/coil) and 2 pole control (3 turns/coil) winding prototype machine. The rotor was of the Broadway cage type. With positive sequence control winding excitation, there were problems with synchronizing the alternator and the excitation requirements were excessive. With negative sequence excitation, the alternator synchronized and at certain operating conditions, the control winding also started generating power. This phenomenon is discussed in detail later. The machine was rewound for the different stator configurations mentioned on page 34. In these configurations, the alternator was not able to generate $14.5V_{dc}$ even at low load currents and in some cases synchronization problems occurred. Overall, the best configuration in terms of low control winding requirements and high efficiency was with 1 turn/coil on the power (6 pole) and 3 turns/coil on the control (2 pole) winding.

When the control winding control winding phase sequence is the same as the power winding sequence, the frequency of the power winding output voltage is

$$f_p = (p_p + p_c)N_s - f_c \qquad \text{-- 3.2.1}$$

This indicates that at a constant mechanical speed, an increase in control winding frequency decreases the power winding frequency. This reduces the reactive voltage drop in the alternator {reactive drop = $2\pi f_p(L_{pm} + L_{lp})$}, where L_{pm} and L_{lp} are as defined in the

Table 3.2.2
Simulation results - 6/2 pole machine
6 pole(1 turn/coil); 2 pole(3 turns/coil)
V_{dc}=14.5V, I_{dc}=10A, f_m=100r/sec

f_2 Hz	I_{2ph} amps.	V_{2ph} volts	Angle degrees	Efficy %
.01	4.91	0.89	-0.11	24.56
10	4.99	1.92	-74.26	25.69
20	5.09	3.79	-88.09	26.86
30	5.21	5.84	-92.94	28.1
40	5.31	8.02	-95.49	29.43

f_2, I_{2ph} and V_{2ph} are the 2 pole frequency, phase current and phase voltage respectively. Angle denotes the 2 pole power factor angle.

Table 3.2.3
Comparison of simulation results - 6/2 and 12/4 pole machine
6 & 12 pole(1 turn/coil); 2 & 4 pole(3 turns/coil)
V_{dc}=14.5V, I_{dc}=10A, f_m=100r/sec

	Prototype 1 6/2 pole machine			Prototype 2 12/4 pole machine		
fc Hz	I_{cph} Amps.	V_{cph} Volts	Efficy %	I_{cph} Amps.	V_{cph} Volts	Efficy %
.01	4.91	0.89	24.6	9.67	4.25	3.7
10	4.99	1.92	25.7	9.85	4.26	4.1
20	5.09	3.79	26.9	10.03	4.61	4.4
30	5.21	5.84	28.1	10.22	5.25	4.8
40	5.31	8.02	29.4	10.42	6.14	5.2

f_c, I_{cph}, V_{cph} are control winding frequency, phase current and phase voltage respectively.

steady-state circuit of Fig. 3.1.1. This reduction in the voltage drop improves the alternator performance. The above observation is also true when the power winding turns/coil are a minimum, which effectively means a low (L_{pm} + L_{lp}). However, a low number of turns per coil reduces the mutual coupling between the power winding and the rotor. This reduction is proportional to the number of turns; whereas the inductance decreases by a factor of turns squared. Thus, the overall performance of the machine improves with low turns/coil on the power winding.

For a given alternator speed and control winding excitation frequency, the reactive drop in the power winding is high when the sum of the power and control winding pole pairs is large, as can be seen from equation 3.2.1. This drop affected the performance of the 12 pole power and 4 pole control winding machine adversely. The predicted control winding requirements were very high and efficiencies low. Table 3.2.3 gives a comparison of the performance of the 6/2 pole machine and 12/4 pole machine for a load current of 10A at 14.5V_{dc}, the alternator speed being 6000r/min. As expected from simulation, an experimental 12/4 pole prototype machine performed poorly and not enough data points could be recorded to present experimental results. A 10 pole power and 2 pole control winding machine was evaluated in the simulation model, and again the results were not encouraging. No prototype was built for this configuration. In the studies conducted, the 6 pole power (1 turn/coil) and 2 pole control (3 turns/coil) winding with the Broadway cage rotor design resulted in the best performing machine; some efficiency predictions at varying speeds and electrical loads are shown in Fig. 3.2.2.

The control winding has to supply most of the magnetizing requirement of the BDFM alternator because the power winding fundamental phase angle is almost unity. For a given MMF, the BDFM alternator current excitation requirement reduces as the number of turns/coil in the control winding is increased. This in turn leads to a cheaper inverter as the rating of the inverter is less. Further, if the control winding excitation phase sequence is the same as the mechanical frequency, then there is the possibility of induction generator operation from the control winding. It has been shown that an induction machine connected to a three phase source will generate power if the mechanical frequency is greater than the supply frequency and that the generation is maximum at frequencies close to the supply frequency[22]. This is shown in Fig. 3.2.3. The control winding of the BDFM alternator exhibits this mode of generation when the control winding excitation frequency is slightly less than the mechanical frequency. Regeneration from the control winding is possible because the inverter transistors have diodes connected in anti-parallel. Further, effective power can be drawn from the control winding only when the generation voltage is large enough to charge the battery (12V) and supply the load.

The above discussion gives good insight into the operation of the BDFM alternator and the design features that need to be incorporated in the design of a stator. The next section discuss rotor design issues.

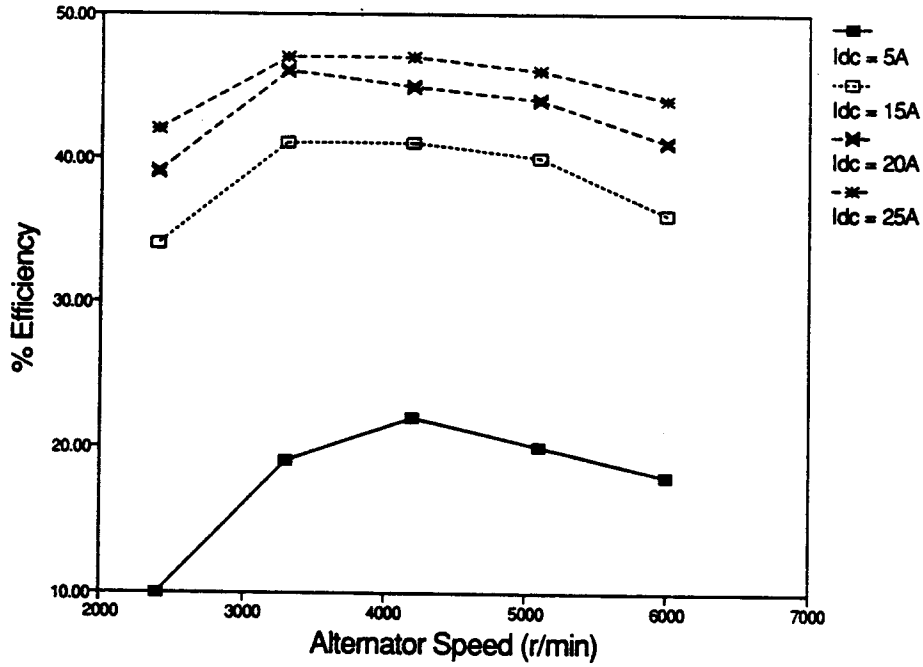

Fig. 3.2.2 Simulation results - BDFM performance

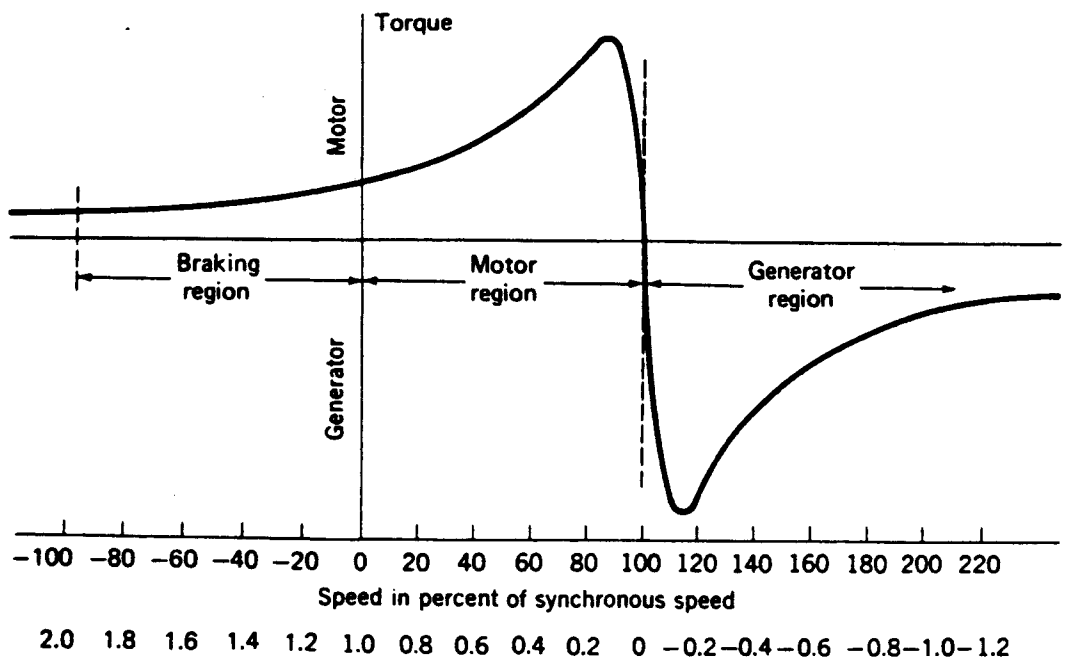

Fig. 3.2.3 Torque - speed curve for induction machine [22]

3.3 Rotor Configurations

Design studies on three different rotor configurations were performed. Representative prototypes were built and tested in the laboratory. All rotor studies utilize the 2hp machine frame with a 6 pole power winding (1 turn/coil - double layer) and a 2 pole control winding (3 turns/coil - double layer). The rotor has 32 slots.

The rotor has to have a cage/loop structure to support both the power and control winding fields. Further, the rotor structure should be easy and inexpensive to manufacture. Three appropriate configurations were investigated: Broadway cage/loop rotor shown in Fig. 3.3.1a; the Broadway rotor without cage shown in Fig. 3.3.1b and the interleaved rotor shown in Fig. 3.3.1c. The goal of the investigation is to identify rotor loop configurations which couple well with both the power and the control winding, thus enhancing overall machine performance. A given power winding current requirement demands an appropriate rotor current and an increase in power winding to rotor coupling allows for lower rotor currents. The rotor current in turn is induced from the control winding current; again, rotor to control winding coupling is inversely proportional to control winding current. The coupling factor (span factor) as a function of the loop span angle is shown in Fig. 3.3.2. For a 6/2 pole machine the loop span angle should be 90 and 180 degrees to couple well with both the 6 and 2 pole windings. This is achieved by the interleaved rotor. However, the accompanying increase in rotor resistance and inductance leads to performance degradation with respect to the other two rotor structures even though the coupling factors are lower in the non-interleaved configurations.

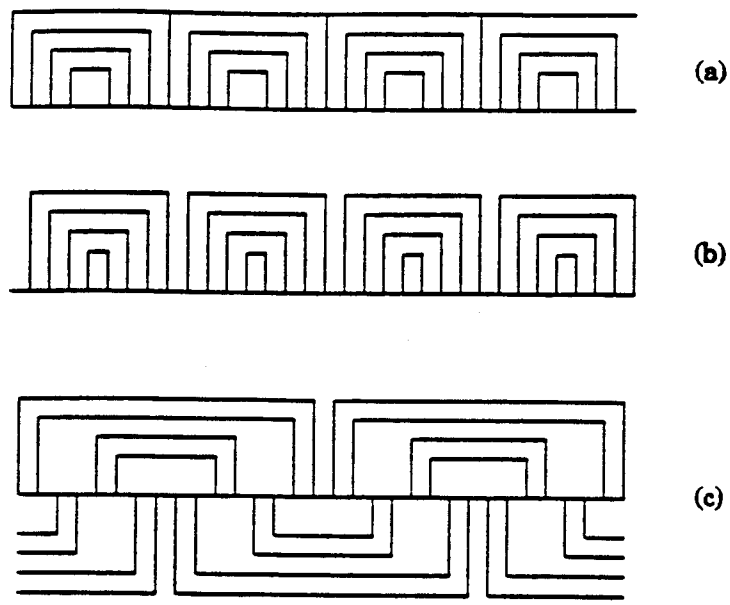

Fig. 3.3.1 Alternative rotor designs
(a) Conventional Broadway; (b) Broadway without cage; (c) Interleaved structure.

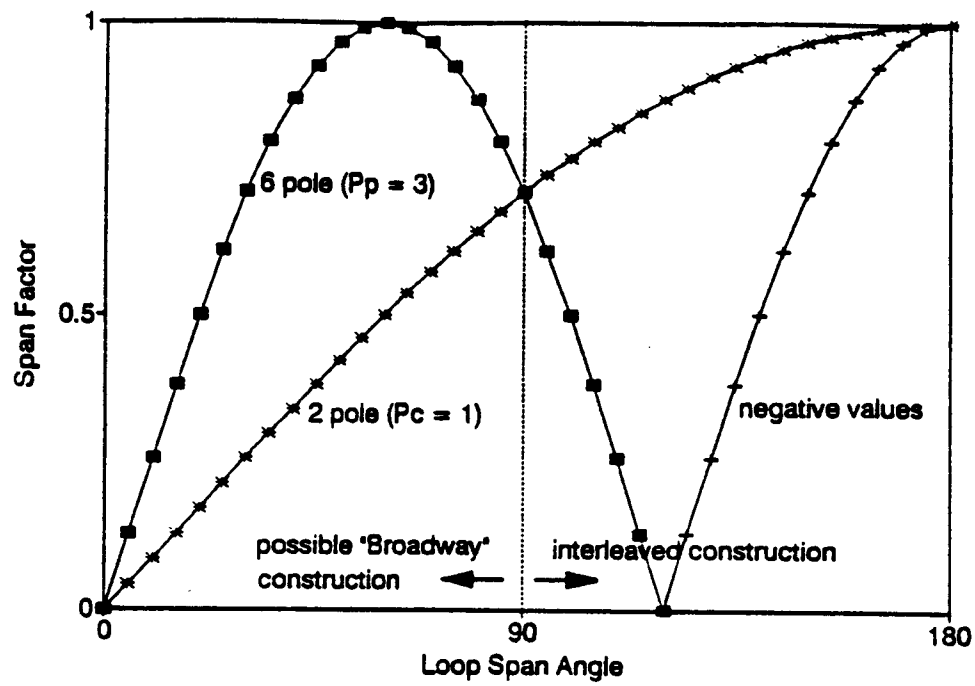

Fig. 3.3.2 Loop span factors

Calculated equivalent steady-state rotor parameters are listed in Table 3.3.1. All parameters are for a single turn power and control winding. Since the stator configuration is the same in the three rotor configurations, the stator parameters (power and control winding resistances and inductances) are the same. As mentioned earlier, the mutual coupling from the power and control winding to the rotor is maximum in the interleaved rotor configuration, but the self-inductance and resistance of the rotor loops are also significantly large. This offsets the advantage of increased coupling. Simulation studies as well as prototype testing indicate that the interleaved rotor leads to an inefficient alternator. Simulation results show that the Broadway cage/loop rotor is the best rotor configuration and this has been verified experimentally using prototype rotors.

Table 3.3.1
Rotor parameters*

	Rotor Option		
Parameter	Broadway	Broadway without cage	Interleaved
M_{6r} - μH	39	36	43
M_{2r} - μH	202	164	336
R_r - $\mu\Omega$	240	216	265
L_{rm} - μH	270	190	646

* Base values for one turn each on 6- and 2-pole stator windings.
M_{6r} 6-pole to rotor mutual coupling.
M_{2r} 2-pole to rotor mutual coupling.
R_r Rotor resistance.
L_{rm} Rotor self inductance.

The Broadway rotor can be die-cast, since the rotor structure is similar to the cage rotor of a conventional induction machine. The resistive losses in the rotor can be reduced considerably by making the common end ring of a bigger dimension than the loop bars. This is because the end ring current is equal to the sum of all the loop currents. Further, the frequency of the current in the rotor depend on the mechanical speed and the stator pole structure by the relationship

$$f_r = f_c + p_c f_m$$

$$= f_p - p_p f_m$$

where f_r, f_m, f_p and f_c are the frequencies of the rotor, mechanical speed, the power winding and the control winding respectively. For a 6 pole power winding and a 2 pole control winding with dc excitation, the rotor frequency is 100Hz if the mechanical frequency is 100 revs./sec. However, with ac excitation on the control winding and with frequencies close to the mechanical frequency the rotor frequencies are very low. The maximum control frequency is limited by the available voltage ($8V_{l\text{-}l}$ for a 12V system). Finite element analysis software is being used to design an efficient rotor for the BDFM alternator by Salim[24].

CHAPTER 4

ALTERNATOR PERFORMANCE RESULTS

The Lundell alternator performance is characterized for varying electrical loads and speeds. Similar tests are performed for the prototype BDFM alternator. Some performance comparisons between the two machines are also presented in this chapter.

The construction of the Lundell alternator was explained in Chapter 1. The off-the-shelf Lundell alternator under test is rated at $14.5V_{dc}$ and 40A dc load current. The stator has 42 slots with a 14 pole, three phase winding connected to a three phase diode rectifier. The rotor winding is wound on an iron core and a chopper regulator circuit via slip rings controls the current in the rotor windings, to maintain 14.5 V_{dc} at the output terminals for all load currents. Fig. 3.1.3 in Chapter 3 explains the test rig configuration used in the laboratory to test the alternators. Machine performance is evaluated at speeds ranging from 2000r/min to 6000r/min, a common automotive alternator speed range.

Test results for the Lundell alternator operating at three different current levels are shown in Fig. 4.1. These results indicate that the peak efficiency of the Lundell system is less than 50% and decreases further at higher speeds. This reduction in efficiency at high speeds can be attributed to the high windage loss rotor. Further, at speeds below 2500r/min and high load currents, the regulation system was not capable of maintaining $14.5V_{dc}$ at the output terminals. The battery then supplies part of the load current, leading to an eventual discharge.

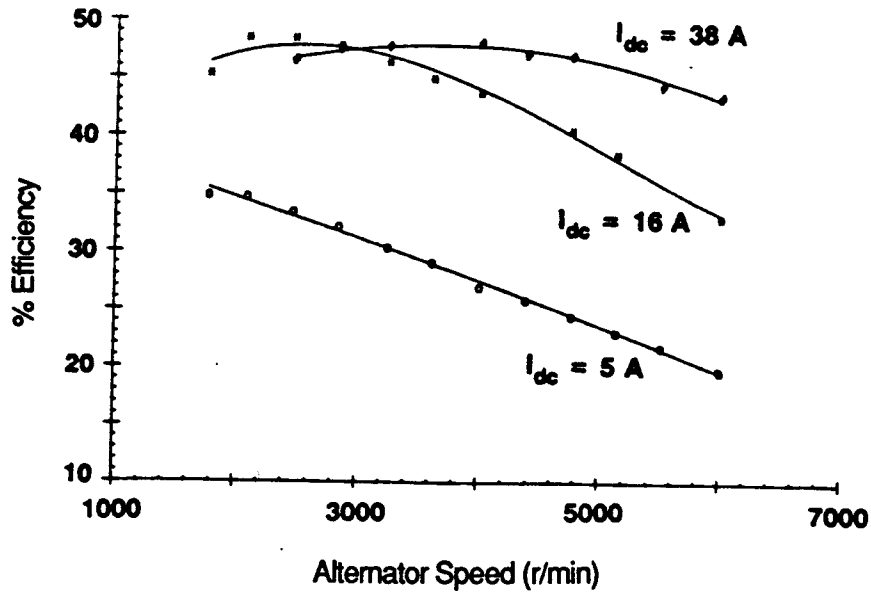

Fig. 4.1 Lundell alternator - Performance characteristics

The prototype BDFM alternator has 36 slots in the stator and has a 6 pole double-layer power winding and a 2 pole double-layer control winding. The power winding has 1 turn/coil and the control winding has 3 turns/coil. The rotor has 32 slots with a Broadway cage/loop type structure with 4 nests and 4 loops/nest. Design studies as described in Chapter 3 identified this machine configuration as optimum. The results of the machine performance for different load currents at different speeds is shown in Fig. 4.2. As explained in previous chapters, the BDFM alternator efficiency at a given operating point can be improved by varying the frequency of the control winding. This feature is evident from Fig. 4.3. The efficiency of the system increases from 28% to 40% when the control winding frequency increases from 55Hz to about 74Hz at an alternator

speed of 6000r/min. The efficiency points in Fig. 4.2 are the maximum efficiencies attainable at a particular operating point.

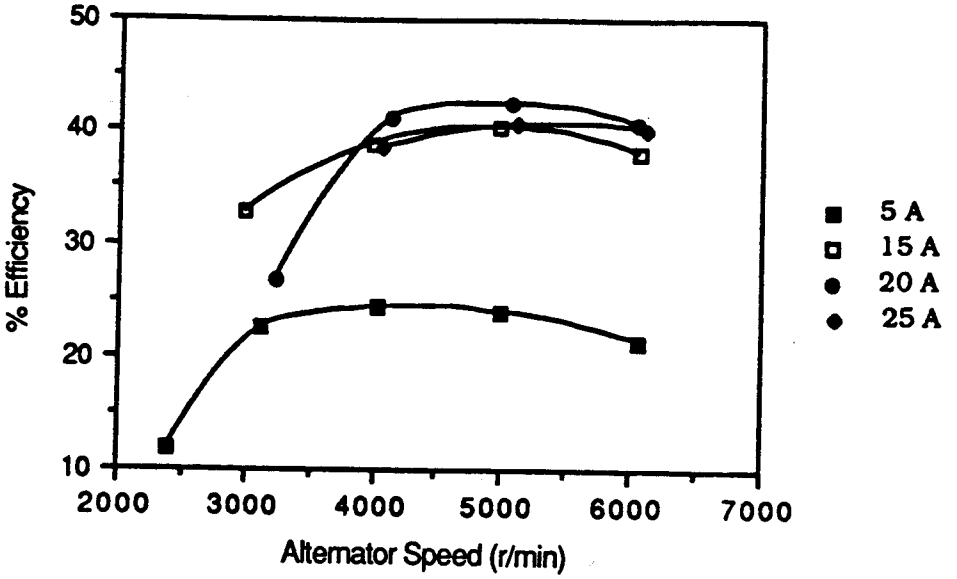

Fig. 4.2 BDFM prototype alternator - Performance characteristics

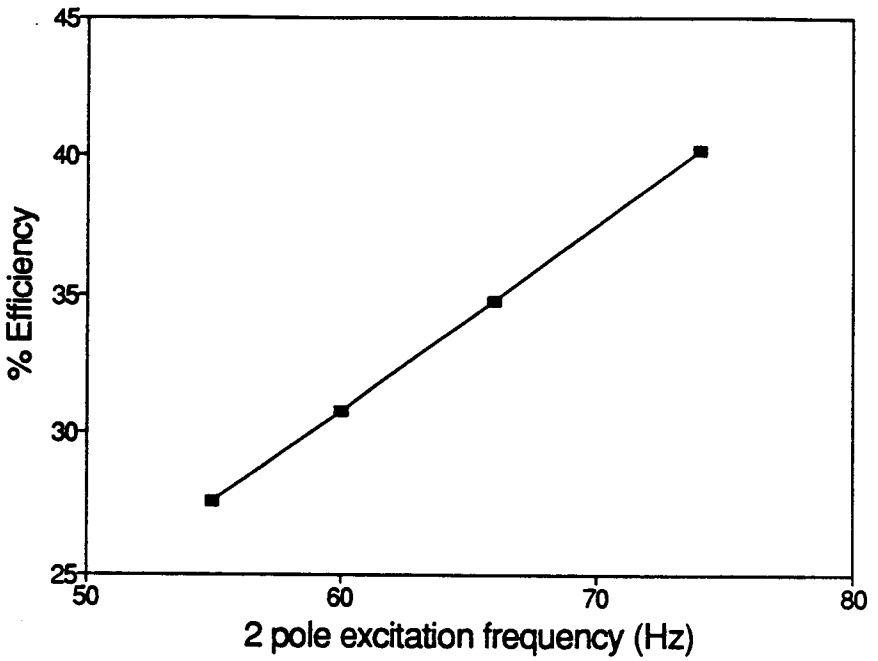

Fig. 4.3 Efficiency maximization principle
(Load current = 20A, Alt. speed = 6000r/min)

The efficiencies cannot be increased over a certain maximum due to the limit on control excitation frequencies. As the control winding excitation frequency increases the impedance also increases, thus limiting the maximum excitation current for the limited inverter output voltage. Moreover, control winding frequency needs to be less than mechanical frequency to enable regeneration through the inverter diodes.

The BDFM simulation model predicted similar results. An increase in system efficiency with increase in control winding frequency is predicted by the model. The correlation of predicted results (Fig. 3.2.2 in Chapter 3) with prototype test results (Fig. 4.2) are acceptable, considering the simplicity of the model. Note that in order to get the quality of predictions shown, the friction and windage loss was adjusted to include loss

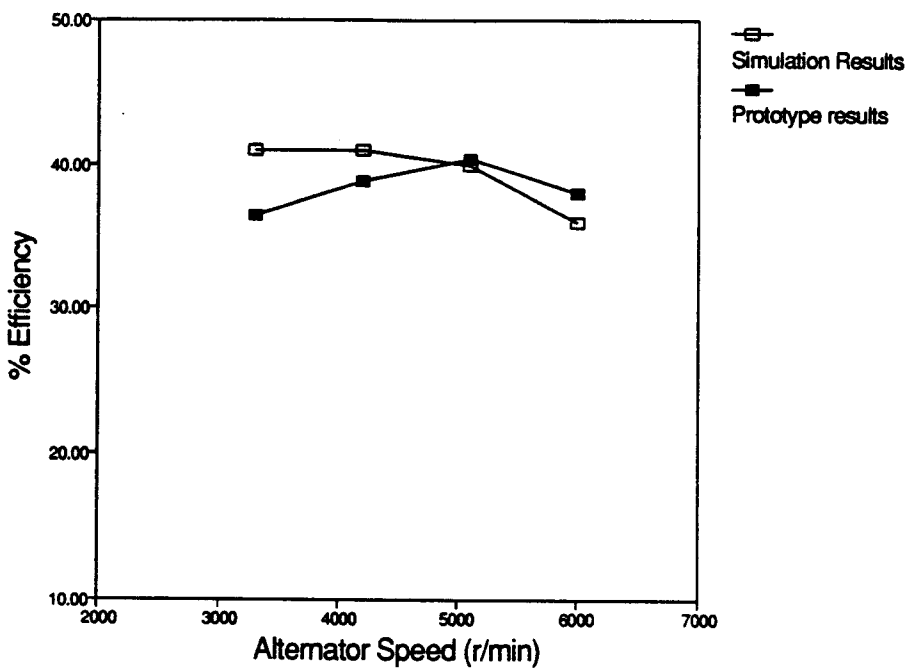

Fig. 4.4 Comparison of simulation and prototype test results (load current=15A)

components not provided for in the model. Fig. 4.4 shows a comparison of prototype machine results with simulation model results at a load of 15A.

Due to the voltage limit on the control winding ($8V_{l\text{-}l(rms)}$), the BDFM alternator was not able to support loads greater than 25A while maintaining an output terminal voltage of $14.5V_{dc}$. Moreover, the maximum efficiencies at load currents below 25A were in the range of 43%. Fig. 4.5 shows a comparison of the efficiencies of the Lundell system and the BDFM alternator system at a load current of 15A. The performance of the BDFM alternator is marginally better at some operating points but overall the results are relatively low. Some of the reasons for these results are discussed below.

The stator design of the prototype machine was based on a conventional 4 pole, 2hp,

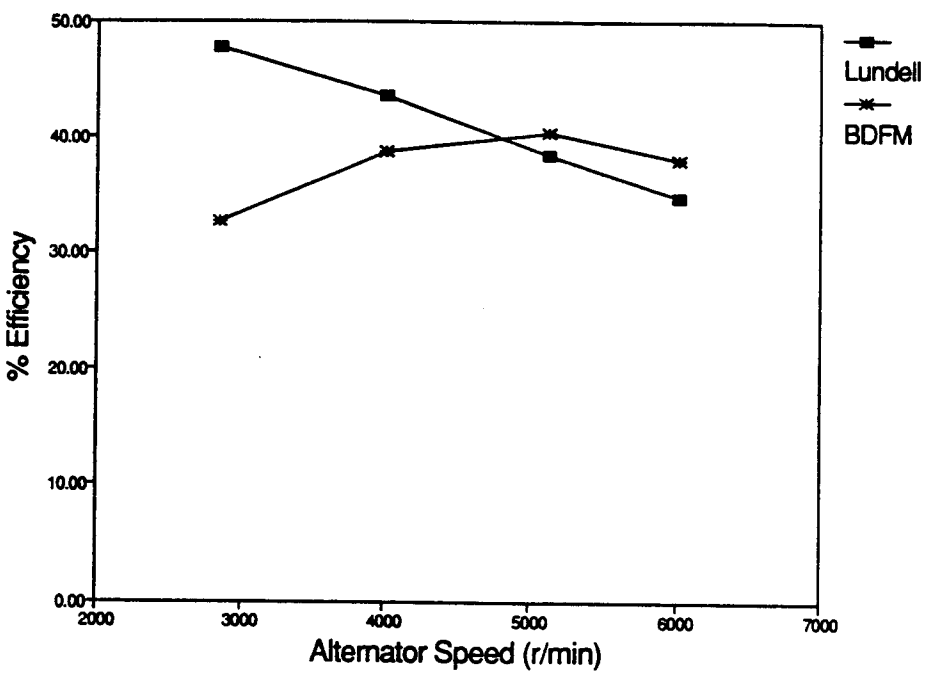

Fig. 4.5 Performance comparison between Lundell and BDFM alternator systems (Load current = 15A)

230V, 60Hz induction machine. The stack length of the stator is much longer than needed for the 15V, 400Hz alternator. The flux levels that need to be maintained for the given alternator rating are much lower and thus the stack length needed is less. This is evident by comparing the stack lengths of the Lundell alternator(0.022m) and the BDFM machine(0.073m), the diameter being about the same. The issue of aspect ratio (i.e. ratio of stack length and diameter) in alternator design is discussed in the next chapter. The result of a longer stack length is an increased magnetizing requirement. Since almost all of the magnetizing current is supplied by the control winding, the control winding requirement increases correspondingly. This requirement cannot be met in this configuration, given the maximum control voltage limitation. Simulation studies indicated that reducing the stack length of the prototype machine by one-half while leaving the rest of the machine parameters the same, would improve performance by as much as 10% in the higher speed and load ranges. The performance parameters for the reduced stack length machine can be derived by appropriate reduction [17] in the inductance and resistance of the prototype machine. Fig. 4.6 shows the improvement in efficiency of the reduced stack length machine at a mechanical speed of 6000r/min and varying electrical loads.

The BDFM configuration requires two three phase windings in the stator. To accommodate the two windings in the stator slot the conductor size of the two windings are much smaller than desired. This leads to increased resistive power losses and voltage drops. Since the control winding voltage is limited the maximum control winding current is also limited. This in turn limits the load current that the power winding can supply.

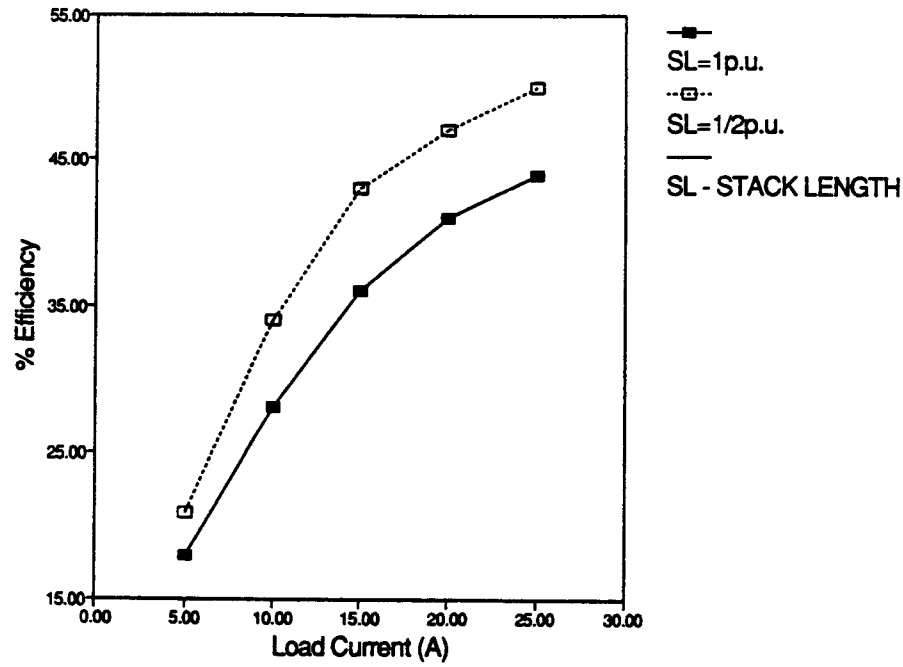

Fig. 4.6 Simulation results for different stack lengths

Since the control winding current is supplied by the power winding, the efficiency of the system is drastically affected.

The power winding frequency varies from about 200Hz to 400Hz. Core losses at these frequencies are a significant percentage of the total loss. The larger than required stack length in the BDFM increases this loss, since core loss is directly proportional to the volume of the material.

The performance results of the BDFM alternator are slightly lower than the performance results of the Lundell system. But the idea behind this thesis is not only to

find a better, more efficient alternative to the Lundell also but to explore the possibility of a higher voltage and higher power rating generation system. A $24V_{dc}$, 2kW BDFM alternator system is proposed in the next chapter.

CHAPTER 5

Design OF A 24V, 2kW BDFM Alternator System

This chapter details the design of a 24V, 2kW BDFM alternator system. This system has a number of advantages over the 12V BDFM system, some of which are discussed later. Some predictions on the performance of this system will be presented in this chapter.

The need to investigate a 2kW, $24V_{dc}$ system is the projected increase in electrically operated equipment in an automobile. The power generating capacity has to increase with increased demand, and the system voltage has to be increased to reduce the current carrying conductor size. The BDFM alternator is better suited for this application than the Lundell machine for a number of reasons discussed below.

In Chapter 1, the construction of the Lundell alternator was discussed. The flux path in the Lundell machine is axial to the shaft, so any increase in the output power capability of the machine can only be achieved by increasing the diameter of the rotor. Because of the claw-pole structure of the rotor, an increase in diameter will increase the friction and windage loss and effect the efficiency drastically. Moreover, increase in rotor diameter is limited for structural reasons and space constraints under the hood.

The BDFM alternator does not share the constraints of the Lundell machine when increasing the power rating. The induced voltage in a BDFM alternator is proportional to

the flux density(B), the diameter at air-gap(d), and the stack length(l). To optimize utilization of the magnetic material, most machines are designed to operate near saturation at rated conditions. Thus, further increase in flux density is not possible. Consequently, either the stack length or the diameter has to be increased in order to increase the power capability of the machine.

As mentioned earlier, an increase in diameter increases the friction and windage loss. Automotive alternators being high speed machines, this loss can be a significant factor in adversely effecting machine performance even with a smooth rotor surface. Further, for large diameter, short stack length machines operating at high speeds, the mechanical tolerances become more stringent as the normal forces increase with speed. However, a large diameter machine could have good sinusoidal output waveforms as more slots can be accommodated in the stator and rotor. A small stack length means less winding resistance which reduces copper losses in the machine. The inductance parameters remain the same if the diameter to stack length ratio (i.e. aspect ratio) remains the same.

A long stack length, small diameter machine would have low friction and windage loss but high copper losses because of increased resistance. A high winding resistance also means high voltage drop across the windings, which also affects machine performance. Given these advantages and disadvantages of the two options, a balance has to be struck to arrive at the best possible alternator design. The space available under the hood will be an important factor in choosing a design.

While the 12V BDFM prototype system showed relatively poor performance, the proposed 24V system is expected to perform better. The most significant advantage of the 24V BDFM system over the 12V BDFM system is the possible increase in the control winding excitation voltage. Since the system voltage is 24V, the alternator output voltage should be about $26V_{dc}$ to charge a 24V battery. This voltage is now the input to the dc-ac inverter feeding the control winding. Thus, instead of a maximum $8V_{l\text{-}l}$rms control voltage available in the 12V system, the 24V system allows for a maximum excitation voltage of $16V_{l\text{-}l}$rms. This allows the system to operate at high control winding frequencies (close to the mechanical frequency) and thereby better efficiencies. Moreover, an increase in stator slot size (within limits dictated by magnetic considerations) helps to accommodate two three phase windings while keeping the resistance of both the windings low. This helps to reduce the voltage drop as well as the power loss in the stator windings.

The proposed 24V BDFM alternator has a stator similar to the 12V machine, a 6 pole power winding and a 2 pole control winding. The physical dimensions of the machine are the same as that mentioned in Chapter 3(Section 3.2, pp27). This is because the diameters of the Lundell and the prototype BDFM are about the same, while the stack length of the BDFM is about 3.5 times the length of the Lundell. Since the power rating of the 24V machine is about four times the rating of the 12V machine, the present prototype should be able to handle the increased power requirement. However, the slots in the stator are bigger than the off-the-shelf induction machine stator, to accommodate two three phase windings of low resistance. The rotor has 32 slots and a 4 nest, 4 loops/nest configuration, described earlier in Fig.(3.3.1a). The stator and rotor are

designed for high frequency operation. After conducting design studies (see Chapter 3) on the 24V system, the most promising alternative has 1 turn/coil on the power winding and 3 turns/coil on the control winding. The steady-state parameters of the 24V BDFM alternator are calculated; performance predictions are discussed in the following.

Fig.(5.1) shows the performance results of the BDFM alternator at four different current levels and different speeds, as predicted by the simulation model. The speed range is from 2400 r/min to 6000 r/min. The efficiency points are the maximum efficiencies possible at the given operating points as predicted by the model. System efficiencies are calculated by considering the losses occurring in the system; the simulation procedure is the same as explained in Section 3.2. The model predicts higher efficiencies for the 24V system and some of the reasons for the high efficiency predictions are discussed below.

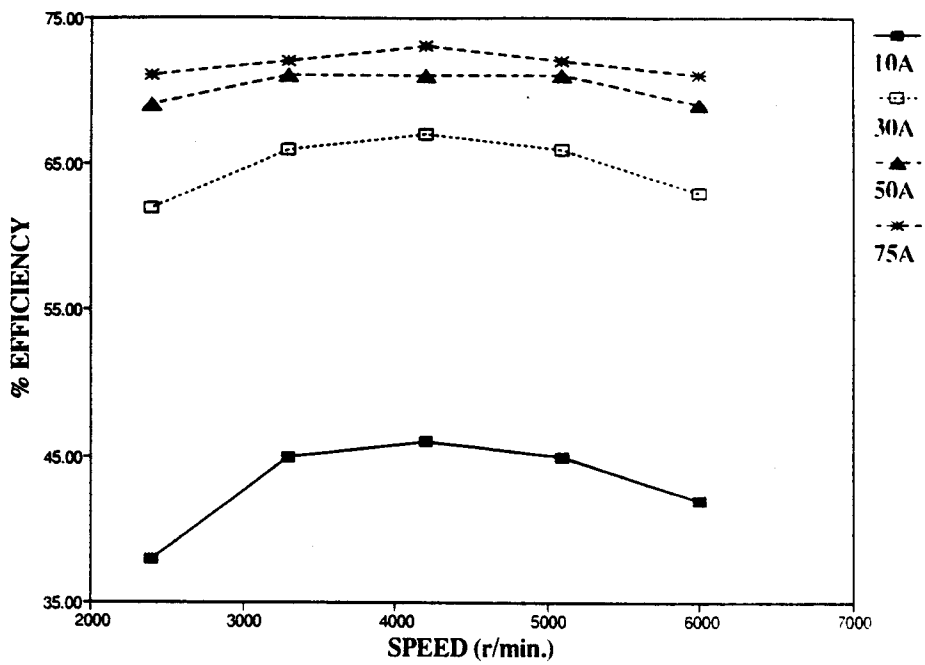

Fig. 5.1 Simulation results for a 24V, 2kW BDFM alternator system

The BDFM alternator is self-excited, and the efficiency of the system increases with reduced control winding excitation. The control winding requirement is reduced by operating the BDFM at control frequencies close to the mechanical frequency, at which point instead of absorbing power the control winding also starts generating. This was not always possible in the 12V system because of the limited control winding voltage, whereas the 24V system permits this at almost all operating points. Another reason for the high efficiency predictions is the higher power rating of the system. The forward drop losses associated with the electronics of the system (inverter and rectifier losses), do not increase with an increase in the voltage rating of the system. Thus, for a given current level, the percentage of losses in the electronics reduces with respect to the power rating and the overall efficiency of the 24V, 2kW system increases.

While the predicted efficiencies are higher than the 12V system efficiencies, they can still be improved upon. The losses in the diode rectifier and the dc-ac inverter can be reduced by using low voltage drop devices. Further, these studies were based on a 6 pole power and 2 pole control winding configuration, which was the best configuration for a 12V system. For a 24V system, different pole combinations can be evaluated for a possible increase in efficiency.

CHAPTER 6

CONCLUSIONS AND RECOMMENDATIONS

The electrical power demand in automobiles is projected to increase from the present level of 600W to about 2-3kW in the near future. This increase in electrical power demand will be due to the increasing use of electrical systems in an automobile. The increasing power demand cannot be met efficiently by the conventional Lundell alternators as was explained in Chapter 1.

The proposed BDFM alternator system is a viable alternative for automotive alternators because of the low cost, robust machine construction and low rating converter. The proof-of-concept prototype BDFM system was designed for a 12V system. While the prototype system could not match the efficiencies of the conventional Lundell system at low speeds, it did better than the Lundell machine at higher speeds (Fig. 4.4, Chapter 4). This is due to the high windage loss rotor structure of the Lundell. The BDFM on the other hand has a smooth surface rotor and performs better at high speeds. The control winding requirements are lower at high speeds. The efficiencies of the BDFM system can be increased by having the control winding excitation frequency close to the mechanical frequency, when the control winding also starts generating. This is the best operating point of operation in terms of system efficiencies. However, this operation was not always possible in the prototype machine because of the limitation in control excitation voltage. The longer than required stack length and the high resistance of the windings compounded the issue, as all the magnetizing requirements are met by the control winding. Further, the

rotor bar geometry used does not lend itself well for high frequency operation. Simulation results indicated an increase in efficiencies by as much as 8% (Fig. 4.5, Chapter 4) when the stack length is reduced by half. The simulation model is based on the steady-state BDFM equivalent circuit and gave good correlation between simulation and prototype test results (Chapter 3 & 4). Improvement in efficiencies is also possible by reducing the losses in the inverter and rectifier by using low voltage drop devices. A low voltage drop in the inverter devices will also increase the voltage availability for the control winding and enable higher control frequency excitation.

As the power requirements in an automobile increases, the voltage level is also expected to increase from the present 12V to 24V, to keep the conductor sizes small. The higher voltage level improves the performance of the BDFM, as illustrated by the 24V, 2kW system proposed in Chapter 5. Comparatively higher efficiencies are projected by the simulation model (Fig. 5.1) for the system, primarily due to the higher voltage available for the control winding allowing maximum efficiency points to be attained, by keeping the control excitation frequency close to the mechanical frequency.

The stator frequencies in the BDFM are in the range of 300-400Hz. Since iron losses increase with frequency, the stator should be designed to keep the iron losses at a minimum. The prototype BDFM machine was built in an available 60Hz induction machine frame and the iron losses were accordingly high. The BDFM stator should also have bigger slots to accommodate two 3-ϕ windings and thus keep the copper losses low.

Recommendations for Future Work:

This thesis work primarily addresses a 6/2 pole machine with some analysis for a 10/2 pole and 12/4 pole machines. Other pole combinations are possible and one promising combination may be a 14/10 pole stator with a 12 nest cage rotor. While the output frequency of this configuration will be in the range of 800-1200Hz and may be a disadvantage in the lower voltage (12V) system, the coupling of the power and control winding to rotor is better in this configuration. Studies should also be performed on high frequency stator design to keep the iron losses low. Studies on rotor bar geometries should address possible reduction in leakage flux and rotor losses at high operating frequencies.

The inverter and rectifier in the alternator system play an important part in improving overall efficiencies, since these losses are a significant percentage of the total power. Packaging the whole controller in a single smart power package and keeping the losses low by using low voltage drop devices will help improve the efficiency of the system further.

BIBLIOGRAPHY

[1] Hunt, L.J. " A New Type of Induction Motor," Journal IEE, vol. 38, pp. 648-667, London, 1907.

[2] Javadekar, V., D.K., Ravi, Spee, R, Wallace, A.K. " A Variable-Speed Brushless Doubly-Fed Automotive Alternator," European Power Electronics Conference, pp. 99-103, Florence, Italy, 1991.

[3] Boules, N. " Performance Requirements for Future Automotive Electrical Machines," Proceedings NSF Workshop on Electrical Machines and Drives, Michigan State University, pp. 16-21, Michigan, 1988.

[4] Mhango, L.M.C. " An Experimental Study of Alternator Performance Using two Drive Ratios and a Novel Method of Speed Boundary Operation," Conf. Rec. IEEE IAS Annual Meeting, Seattle, pp. 301-308, 1990.

[5] Wang, R and Demerdash, N.A. " Extra High Speed Modified Lundell Parameters and Open/Short-Circuit Characteristics from Global 3D-FE Magnetic Field Solutions," IEEE PES Winter Meeting, New York, paper 91WM067-9EC, 1991.

[6] King, R.D. " Combined Electric Starter and Alternator System using a Permanent Magnet Synchronous Machine," US Patent No. 4,862,009.

[7] Rochelle, P.R. " Program "BDFM" User's Manual," Oregon State University, 1991.

[8] Li, R., Wallace, A.K., Spee, R. and Wang, Y. " Two-Axis Model Development of Cage-Rotor Brushless Doubly-Fed Machines," IEEE PES Winter Meeting, New York, paper 91WM061-2EC, 1991.

[9] Creedy, F. " Some Developments in Multi-Speed Cascade Induction Motors," Journal IEE, vol. 59, pp. 511-521, London.

[10] Broadway, A.R.W. and Burbridge, L. " Self-Cascaded Machines: A Low Speed Motor or High Frequency Brushless Alternator," Proc. IEE, vol. 117, pp. 1277-1290, 1970, London.

[11] Cook, C.D. and Smith, B.H. " Stability and Stabilization of Doubly-Fed Single Frame Cascade Induction Machine," IEE Proc., vol. 126, pp. 1168-1174, 1979.

[12] Kusko, A. and Somah, C.B. " Speed Control of a Single Frame Cascade Induction Motor with Slip-Power Pump Back," IEEE Trans. on IAS, vol. IA-14(2), pp. 97-105, 1978.

[13] Spee, R., Wallace, A.K. and Lauw, H.K. " Simulation of Brushless Doubly - Fed Adjustable Speed Drives," Conf. Rec. IEEE IAS Annual Meeting, pp. 738-743, 1989.

[14] Rochelle, P.R., Spee, R. and Wallace, A.K. " The Effects of Stator Winding Configuration on the Performance of Brushless Doubly-Fed Machines in Adjustable Speed Drives," IEEE IAS Annual Meeting, Seattle, Wash., Oct. 8-11, 1990.

[15] Wallace, A.K., Rochelle, P.R. and Spee, R. "Rotor Modelling and Development for Brushless Doubly-Fed Machines," International Conf. on Electric Machines, vol. 1, pp. 54-59, Cambridge, MA, 1990.

[16] Alexander, G.C. " Characterization of the Brushless Doubly-Fed Machine by Magnetic Field Analysis," IEEE IAS Annual Meeting, Seattle, Wash., Oct. 8-11, 1990.

[17] Li, R., Wallace, A.K. and Spee, R. "Dynamic simulation of Brushless Doubly-Fed machine," IEEE Trans. on Energy Conversion, vol. 6, pp. 445-452, 1991.

[18] Lauw, H.K., Klassens, J.B., Butler, N.G. and Seely, D.M. "Variable-Speed Generation with the Series Resonant Converter," IEEE Trans. on Energy Conversion, vol. 3, pp. 755-764, 1988.

[19] Rochelle, P.R. " Analysis and Design of the Brushless Doubly-Fed Machine," Master's Thesis, Oregon State University, 1990.

[20] Mohan, N., Undeland, T.M. and Robbins, W.P. "Power Electronics: Converters, Applications & Design ," John Wiley & Sons, Inc. 1989

[21] Javedakar, V. "Design and Development of a Controller for BDFAA system," Master's Thesis, Oregon State University, 1992

[22] Fitzgerald, A.E., Kingsley, Charles and Umans, S.D. "Electric Machinery," McGraw-Hill, Inc. 1990

[23] Layne, K "Automotive Electronics and Basic Electrical Systems," John Wiley & Sons, Inc. 1990.

[24] Salim, A.M. and Spee, R. "High Frequency Cage Rotor Design" IEEE IAS Annual Meeting, 1992.

APPENDICES

APPENDIX I

STEADY-STATE PROGRAM LISTING

Steady-State Program Listing - Fortran Code

```
      program carbdfm
c     program to calculate the 2 pole current(ic),the 2 pole voltage(vc),
c     the efficiency and the rotor current(iar)
c     ia is 6 pole current, va is 6 pole phase voltage, f6 is 6 pole
c     frequency, f2 is 2 pole frequency, fm is the mechanical speed in
c     revs/sec and fcr is the frequency of the rotor current.
c     Vph2 and iph2 are the phase voltage and current of the control winding.
c     vdc and idc are the dc load voltage and total dc current. dc1 is the
c     the dc load current.
c     ang6 is the phase angle between the power winding voltage and current.
c     icang, vcang and iarang are the phase angles of the control winding
c     current, voltage and rotor current with respect to the power winding
c     voltage phasor.
c     z,z1,z2.... are complex program variables

      complex iar,z,z1,z2,z3,z4,z5,ic,vc,v6,aia,zj
      real ia,icang,iarang,ll1,l1,lm6,ll2,l2,lm2,llr,lr,idc,iph2
     *,f6,f2,fm,k

      open(unit=2,file='car.dat')
c     car.dat has the steady - state parameters of the machine (resistance,
c     self and mutual inductance)

      pi=4.*atan(1.)

      write(*,100)
100   format(2x,'input mechanical frequency and dc load current')
      read*,fm,idc

c     read in the steady - state parameters of the machine
      read(2,*)r1,ll1,l1,lm6,r2,ll2,l2,lm2,rr,llr,lr

c     r1 is the resistance of the power winding, ll1 & l1 are the leakage and
      self inductance of the power winding and lm6 is the mutual inductance
      between the power and rotor windings.

      vdc=14.5
c     convert output dc voltage and current to complex steady-state form
      va=sqrt(1.5)*vdc*pi/(3.*sqrt(6.))+1.5
      ang6=-200.
      ang6=ang6*pi/180.
```

```
      ia=sqrt(1.5)*0.816*idc
      aia=cmplx(ia*cos(ang6),ia*sin(ang6))
      v6=cmplx(va,0.)

      write(3,200)vdc,idc,fm,ang6
200   format('vdc=',f7.3,3x,'idc=',f8.3,3x,'fm=',f8.3,3x,'ang6=',f8.3)
      write(3,300)
300   format(5x,'f2',7x,'I2ph',4x,'V2ph',4x,'phang(vc)',4x,
     *'iar',3x,' effcy ',3x,'ID')
      write(4,500)
500   format(5x,'f2',7x,'l6p',4x,'l2p',7x,'lorr',4x,'lf&w',4x,
     *'ldiod',3x,'linv',3x,'lossf')
      do 11 i=1,100
c     sweep control winding frequencies from almost dc to mechanical frequency
      k=k+1.
       if(k.EQ.1.)f2=-.01
        if(k.EQ.2.)f2=-10.
          if(k.GT.2.)then
              f2=f2-10.
               if(abs(f2).eq.fm)goto 35
          endif

c     change rotor resistance with rotor frequency.
      rr1=((fm-abs(f2))/200.)*rr+rr

c     set up steady - state equations
      f6=(4.*fm)+f2
      fcr=f6-3*fm
      xl1=2.*pi*f6*ll1
      x1=2.*pi*f6*l1
      xm6=2.*pi*f6*lm6
      xl2=2.*pi*f6*ll2
      x2=2.*pi*f6*l2
      xm2=2.*pi*f6*lm2
      xlr=2.*pi*f6*llr
      xr=2.*pi*f6*lr
      s=f2/f6
      s1=(f2+fm)/f6
c     the general formula is s1=(f2+(control poles)/2.*fm)/f6
      ax1=xl1+x1
      z=cmplx(r1,ax1)
      z1=cmplx(0.,xm6)
      ar2=r2/s
      ax2=xl2+x2
      z2=cmplx(ar2,ax2)
```

```
      z3=cmplx(0.,xm2)
      ar4=rr1/s1
      ax4=xlr+xr
      z4=cmplx(ar4,ax4)
      z5=z1


c     calculate control winding voltage and current, rotor current,
c     and the net output dc current

      iar=((v6-z*aia)/z1)
      ic=((z4*iar+z5*aia)/z3)
      vc=((s*z2*ic)-(s*z3*iar))
      icang=atan2(aimag(ic),real(ic))*180./pi
      vcang=atan2(aimag(vc),real(vc))*180./pi
      iarang=atan2(aimag(iar),real(iar))*180./pi
      iph2=cabs(ic)*sqrt(2./3.)
      Vph2=cabs(vc)*sqrt(2./3.)
      dc1=idc-((3.*vph2*iph2*cos(pi/180.*(vcang-icang)))/vdc)

c     subroutine to calculate efficiency
      call efficy(effccy,aia,vdc,idc,ic,iar,r1,r2,rr1,fm,pi,f2,dc1,f6)

      if(Vph2.GT.8.)goto 35
      write(3,400)f2,iph2,Vph2,vcang-icang,cabs(iar)*sqrt(2./3.),effccy
     *,dc1
400   format(7f9.3,f12.9)

11    continue
35    write(3,*)
      end
```

```
c     subroutine efficy calculates the output power, losses and efficiency of the system
      subroutine efficy(effccy,aia,vdc,idc,ic,iar,r6,r2,rr1,fm,pi,f2
     *,dc1,f6)
      implicit real(a-z)
      complex ic,iar,aia,v6

c     calculate output power
      elout=vdc*dc1
```

```
c     calculate losses in the machine
c     loss2p, loss6p and lossrr are the control winding, power winding and rotor
c     copper losses.
c     lossf is the core loss and lossfr is the friction and windage loss.
c     lossd and lossinv are the diode bridge and inverter losses.
      loss2p=cabs(ic)**2*r2
      loss6p=cabs(aia)**2*r6
      lossrr=cabs(iar)**2*rr1
      k=1.3-(.002*f6)
      lossf=115.3/k
      lossd=1.4*cabs(aia)*1.732
      lossfr=4.E-07*(2.*pi*fm)**3
      lossinv=cabs(ic)*2.*1.732
c     calculate total loss in the system
      loss=2.*(loss6p+loss2p+lossrr)+lossf+lossd+lossfr+lossinv

c     calculate efficiency
      effccy=elout/(elout+loss)*100.
      return
      end
```

****

CAR.DAT

Steady-state parameters for 6/2 pole machine
6 pole winding(1 turn/coil); 2 pole winding(3 turns/coil)

.022	r1 - Ω power winding resistance
2.E-05	ll1 - H power winding leakage inductance
2.2E-04	l1 - H power winding self inductance
3.89E-05	lm6 - H power winding to rotor mutual inductance
.18	r2 - Ω control winding resistance
1.8E-03	ll2 - H control winding leakage inductance
1.72E-02	l2 - H control winding self inductance
6.06E-04	lm2 - H control winding to rotor mutual inductance
2.4E-04	rr - Ω rotor resistance
2.99E-06	llr - H rotor leakage inductance
2.69E-05	lr - H rotor self inductance

****

APPENDIX II

Input Data File for Program BDFM

Once stator and rotor geometries are determined, this data file can be generated. The machine in this example has a double layer 6/2 pole structure. There are 4 nests and 4 loops/nest in the rotor. The machine has a 36 slot stator and a 32 slot rotor and the input data file for "Program BDFM" is listed below.

```
0.07   stack length in meters
0.1125  diameter of machine at air gap in meters
0.0005  length of air gap in meters
.00273, .008125          STATOR COIL RESISTANCE
-54.65    RESISTANCE OF "MUTUAL BAR"
125.70,  8.20,  8.20,  8.20  resistance of the rotor
158.49, 24.59, 24.59         loops and the
191.28, 40.99                common ring resistance;
224.07                       refer fig. 2.5.
3.     # of pole pairs of the power winding
1,   0.,    40.,  1.,  1.,  coil 1; start; span; polarity; turns
2,   10.,   40.,  1.,  1.,  coil 2; start; span; polarity; turns
3,   60.,   40., -1.,  1.,  coil 3; start; span; polarity; turns
4,   70.,   40., -1.,  1.,  coil 4; start; span; polarity; turns
5,   120.,  40.,  1.,  1.,  coil 5; start; span; polarity; turns
6,   130.,  40.,  1.,  1.,  coil 6; start; span; polarity; turns
7,   180.,  40., -1.,  1.,  coil 7; start; span; polarity; turns
8,   190.,  40., -1.,  1.,  coil 8; start; span; polarity; turns
9,   240.,  40.,  1.,  1.,  coil 9; start; span; polarity; turns
10,  250.,  40.,  1.,  1.,  coil 10; start; span; polarity; turns
11,  300.,  40., -1.,  1.,  coil 11; start; span; polarity; turns
12,  310.,  40., -1.,  1.,  coil 12; start; span; polarity; turns
1.,    # of pole pairs of the control winding
1,   0.,   120.,  1.,  1.,  coil 1; start; span; polarity; turns
2,   10.,  120.,  1.,  1.,  coil 2; start; span; polarity; turns
3,   20.,  120.,  1.,  1.,  coil 3; start; span; polarity; turns
4,   30.,  120.,  1.,  1.,  coil 4; start; span; polarity; turns
5,   40.,  120.,  1.,  1.,  coil 5; start; span; polarity; turns
6,   50.,  120.,  1.,  1.,  coil 6; start; span; polarity; turns
7,  180.,  120., -1.,  1.,  coil 7; start; span; polarity; turns
8,  190.,  120., -1.,  1.,  coil 8; start; span; polarity; turns
9,  200.,  120., -1.,  1.,  coil 9; start; span; polarity; turns
10, 210.,  120., -1.,  1.,  coil 10; start; span; polarity; turns
11, 220.,  120., -1.,  1.,  coil 11; start; span; polarity; turns
12, 230.,  120., -1.,  1.,  coil 12; start; span; polarity; turns
```

```
4     # of loops per nest of rotor
1.,   22.50  loop 1; span
2.,   45.00  loop 2; span
3.,   67.50  loop 3; span
4.,   90.00  loop 4; span
 1., 0., 0., 0., 0., 0.    ROW1
 0., 1., 0., 0., 0., 0.    ROW2  MATRIX TO
 0., 0., 1., 0., 0., 0.    ROW3  DETERMINE SUPPLY
 0., 0., 0., 1., 0., 0.    ROW4  CURRENTS FROM COILS
 0., 0., 0., 0., 1., 0.    ROW5
 0., 0., 0., 0., 0., 1.    ROW6    ABC abc
 1., 0., 0., 0., 0., 0.       ROW1
 0., 1., 0., 0., 0., 0.       ROW2
 0., 0., 1., 0., 0., 0.       ROW3      MATRIX TO DETERMINE
 0., 0., 0., 1., 0., 0.       ROW4      COIL GROUP VOLTAGES
 0., 0., 0., 0., 1., 0.       ROW5      FROM SUPPLY VOLTAGES
 0., 0., 0., 0., 0., 1.       ROW6
```

APPENDIX III

STEADY-STATE PARAMETER CALCULATION

The steady-state program needs the parameters of the machine to solve the steady-state equations. The parameters that need to be calculated are the resistance and inductance (self and mutual) for both the stator windings and the rotor resistance and inductance. The generalized dynamic simulation program "Program BDFM" is used extensively to generate the parameters. "Program BDFM" generates the abc domain parameters and these are transformed into the d-q domain using the transformation matrices given in References [8,17]. The input data file for "Program BDFM" contains all the information about the stator and rotor structure and the program uses this information to generate the stator and rotor inductance matrices. The parameters are calculated for a single turn/coil power and control winding and later updated as the turns are changed.

Parameter Calculation:

Stator

- Resistance: The power and control winding phase resistances are calculated from wire tables. The phase resistances are transformed to the d-q domain by using the stator transformation matrix in Reference [8]. The transformation matrix does not change with a change in pole number combinations, but changes as the number of phases change. Since, the systems considered were all 3-ϕ systems the transformation matrix remains the same.

- Self Inductance: "Program BDFM" generates phase inductances for both the power and control winding. These inductance matrices are transformed to the d-q domain

using the stator transformation matrix.

- Mutual Inductance: A modified version of "Program BDFM" is used to generate the mutual inductance of a stator phase to all the loops in a nest of the rotor. The fundamental component of the mutual is then evaluated by Fourier analysis. The mutual inductance is calculated according to the expression given below:

$$M_p = k(\sum_i M_{sri}) \text{ where } k = (\sqrt{3}/n)m/2.$$

m is the number of nests and n is total number of loops in the rotor. M_{sri} is the mutual of a stator phase to a loop of the rotor. M_p is the equivalent d-q mutual inductance.

Rotor

- Resistance: The resistance of each loop including the common bar is calculated from the wire table and is an input to "Program BDFM". For a 4 nest rotor, the loop resistance can be transformed to an equivalent d-q resistance by the expression given below:

$$r_r = (1/p)[\sum_i r_i + \sum_j \sum_i r_{ij}]$$

where r_r is the equivalent d-q rotor resistance and r_i and r_{ij} represent the rotor loop and endring resistances respectively. i and j are the loop numbers in a nest and p is the total number of loops in a nest.

- Self Inductance: "Program BDFM" calculates the self inductance of each loop and the mutual inductance of every loop with respect to every other loop in the rotor. The equivalent d-q inductance for a 4 nest rotor can be calculated with the expression given

below:

$$L_r = (1/p)[\sum_{i}(L_i + M_{ii}) + \sum_{j}\sum_{i}(M_{ij} + M'_{ij})]$$

where L_i is the loop self inductance, M_{ii} is the mutual inductance of similar loops in different nests. M_{ij} and M'_{ij} are the mutual inductance between different loops of the same nest and between different loops of different nests, respectively.

While the rotor parameter calculations look very involved, these calculations can be simplified by doing the transformations by matrix manipulation. Reference [8] has the rotor transformation matrices; the abc domain rotor resistance and inductance matrices are generated by "Program BDFM".